THEORY OF RADIATIONLESS TRANSITIONS FORMALDEHYDE AS AN EXAMPLE

THEORY OF RADIATIONLESS TRANSITIONS

FORMALDEHYDE AS AN EXAMPLE

JOHANNES MARIA FRANCISCA VAN DIJK

GEBOREN TE EINDHOVEN

DIT PROEFSCHRIFT IS GOEDGEKEURD DOOR

DE PROMOTOREN

PROF. DR. H.M. BUCK

EN

DR. J.J.C. MULDER

"Die Entwicklung der Wissenschaft löst das "Bekannte"
 immer mehr in ein Unbekanntes auf: - sie *will* aber gerade
 das *Umgekehrte* und geht von dem Instinkt aus das Unbe-
 kannte auf das Bekannte zurückzuführen".

Friedrich Nietsche

0. INTRODUCTION

The rate of radiationless decay is measured by exciting a molecule with electromagnetic radiation and detecting the fluorescence radiation as a function of time; this will give us the fluorescence lifetime τ_F. From the integrated absorption band one can derive the radiative lifetime τ_r with the Strickler-Berg formulas[1-3]. By measuring the ratio of absorbed and emitted radiation one obtains the fluorescence quantum yield ϕ_f. The non-radiative lifetime τ_{nr} can now be derived from:

$$\tau_{mn} = \tau_F / (1 - \phi_f) \quad or \; from \quad 1/\tau_F = 1/\tau_r + 1/\tau_{mn}$$

So this provides even a double-check on the determination of τ_{mn}; however, τ_r is difficult to determine.

Radiationless processes occur in a very wide range of phenomena in the gas, liquid and solid phase. We are especially interested in radiationless transitions because of their wide occurrence in photochemical reactions. Here we will only be concerned with the gas phase and in particular with circumstances in which we can consider the molecules as isolated. In the last couple of years, with the advent of dye LASER technology, many detailed measurements have been made on very low pressure (0.1 Torr) gases. The theoretical activity concerning radiationless processes is also of rather recent origin. Only in 1968, by the work of Bixon and Jortner[4], it was understood that radiationless decay in isolated molecules can occur by means of quantum-mechanical interference of the initial states. Since then a welter of "formal" treatments has showered

down on this area. One of the problems receiving much
attention was which coupling "caused" the radiationless
transition. In Chapter 1 of this thesis this problem is
considered. Only very few people have attempted an actual
calculation of the radiationless process[5]; however, the
quantitative numbers for coupling and density of states
have a decisive influence on the qualitative behaviour of
the system (exponential decay or oscillatory behaviour,
etc.). The calculation of the radiationless process in
formaldehyde, described in this thesis, constitutes the
first such calculation on the *ab initio* level.
In Chapter 2 the formal equations for describing the radia-
tionless process are described. In Chapter 3 these are
applied to formaldehyde. In Chapter 4 we compare the results
for the radiative and non-radiative process with the ex-
periment.

1. THEORY OF RADIATIONLESS TRANSITIONS

1.1. <u>The Exact Description</u>

The time-dependent behaviour of an excited molecule can be completely described with the time-dependent Schrödinger equation:

$$i \frac{\partial}{\partial t} \psi(\vec{r}, t) = H \psi(\vec{r}, t) \tag{1.1}$$

H is the total molecular Hamiltonian; $\psi(\vec{r}, t)$ is the total wave function containing both nuclear and electron coordinates.

We can expand $\psi(\vec{r}, t)$ in some complete set of orthonormal functions $u_n(\vec{r})$:

$$\psi(\vec{r}, t) = \sum_n a_n(t) \cdot u_n(\vec{r}) \tag{1.2}$$

Substitution in (1.1) gives after multiplication with $u_m^*(\vec{r})$ and integration over $\vec{r}$:

$$i \frac{\partial}{\partial t} a_m(t) = \sum_n H_{mn} a_n(t) \ , \quad m = 0, 1, 2, \dots \tag{1.3}$$

where $\quad H_{mn} = \langle u_m(\vec{r}) | H | u_n(\vec{r}) \rangle$

This is a set of coupled linear differential equations.
Substitute:

$$a_n(t) = a_n e^{-iEt}$$

Then:

$$\sum_n (H_{mn} - E \cdot \delta_{mn}) \cdot a_n = 0 \quad , \quad m = 0, 1, 2, \dots \tag{1.4}$$

Solution gives: eigenvalues $E_0, E_1, \ldots, E_k, \ldots$

eigenvectors $\underline{a}_0, \underline{a}_1, \ldots, \underline{a}_k, \ldots$

with $\quad \underline{a}_k = \begin{pmatrix} (a_k)_0 \\ (a_k)_1 \\ \vdots \\ (a_k)_n \end{pmatrix}$

So the solution of (1.1) is: $\quad \psi_k = \sum_m (a_k)_m \cdot e^{-iE_k t} \cdot \mu_m(\vec{r})$ (1.5

The general solution is a linear combination of these solutions, with coefficients α_k determined by $\psi(\vec{r},0)$:

$$\psi(\vec{r},t) = \sum_k \alpha_k \cdot \sum_m (a_k)_m \cdot e^{-iE_k t} \cdot \mu_m(\vec{r}) \quad \longrightarrow$$

(1.6

$$\psi(\vec{r},t) = \sum_m \left\{ \sum_k \alpha_k (a_k)_m \cdot e^{-iE_k t} \right\} \cdot \mu_m(\vec{r})$$

A special case occurs if the $u_n(\vec{r})$ are eigenfunctions of H. Then $(a_k)_n = \delta_{kn}$ and (1.6) reduces to:

$$\psi(\vec{r},t) = \sum_k \alpha_k \, e^{-iE_k t} \cdot \mu_k(\vec{r})$$

(1.7

This case is of value because of the greatly simplified formulas that result from it.

As we are interested in interaction of an excited state ψ_1 with the electromagnetic field, we will consider one component of the oscillator strength f with the ground state:

with:

$$\psi_0 = e^{-iE_0 t} \cdot \mu_0(\vec{r}) = \mu_0(\vec{r}) \quad with \quad E_0 = 0$$

(1.8

$$\psi_1 = \sum_k \alpha_k \, e^{-iE_k t} \cdot \mu_k(\vec{r})$$

$$f_x \sim \left| \langle \bar{\Psi}_o / x / \bar{\Psi}_1 \rangle \right|^2 = \left| \langle \mu_o(\vec{x}) / x / \sum_k \alpha_k \, \ell^{-i E_k t} \, \mu_k(\vec{x}) \rangle \right|^2$$

$$= \left| \sum_k \alpha_k \, \ell^{-i E_k t} \, \langle \mu_o(\vec{x}) / x / \mu_k(\vec{x}) \rangle \right|^2 \qquad (1.9)$$

$$= \left| \sum_k A_{ok} \, \ell^{-i E_k t} \right|^2 \quad \text{with } A_{ok} = \alpha_k \langle \mu_o(\vec{x}) / x / \mu_k(\vec{x}) \rangle$$

So
$$f_x \sim \left(A_{o1} \, \ell^{-i E_1 t} + A_{o2} \, \ell^{-i E_2 t} + \cdots \right) \left(A_{o1}^* \, \ell^{+i E_1 t} + A_{o2}^* \, \ell^{+i E_2 t} + \cdots \right)$$

$$= \sum_k |A_{ok}|^2 + \sum_{k \neq \ell} \sum A_{ok} A_{o\ell}^* \, \ell^{-i(E_k - E_\ell)t} \qquad (1.10)$$

$$= \sum_k A_{ok}^2 + 2 \sum_{k < \ell} \sum A_{ok} \cdot A_{o\ell} \cdot co \, (E_k - E_\ell)t$$

where in the last step the A_{0k} are supposed to be real.
So the oscillator strength is time-dependent if more than
one A_{0k} is unequal zero, *i.e.* if the bandwidth of the ex-
citing radiation exceeds the energy difference between two
contiguous eigenstates of H.
After a certain time, the recurrence time t_R, f will have
the same value as on t = 0; between t = 0 and t = t_R, f
will be less than on t = 0, f can even become practically
zero, especially so if there are many eigenstates involved.
The recurring of the oscillator strength is referred to as
a quantum beat, these have been experimentally observed[1].
As a result of the interference process the lifetime of the
excited state is increased because the oscillator strength
temporarily decreases. The quantum yield, *i.e.* the ratio of
emitted and absorbed radiation, should be unity, however,
despite this behaviour. In the experimental practice this
is often not the case, because the molecule can dissipate
its energy in other ways: collisions with other molecules
or the wall, IR transitions.

With the theory of Bixon and Jortner[2], the different cases
of interference behaviour can easily be recognized and a
classification scheme has accordingly be outlined by Jort-
ner and Berry[3].

1.2. Splitting the Hamiltonian

    We will first digress somewhat upon the possible
choices for $u_n(\vec{r})$, the complete set of functions.
If we take for the $u_n(\vec{r})$ the exact eigenfunctions of H, we
get of course the simplest formulas (see 1.7), but the
exact eigenfunctions are the most difficult to determine,
so we have to resort to sets $u_n(\vec{r})$ that give rise to com-
plicated formulas, but can be easily determined.
In fact we are not interested in describing the total eigen-
value spectrum of H with the basis set $u_n(\vec{r})$, because in
the experimental set-up for measurement of radiationless
transitions, the exciting radiation has a very narrow fre-
quency distribution. So the set $u_n(\vec{r})$ does not have to be
complete. What we will do is derive what portion of the
eigenvalue spectrum of H is described correctly by this
set.
In the model of Bixon and Jortner[2] some extra conditions
are imposed on the set $u_n(\vec{r})$; the validity of these condi-
tions makes it possible to derive the rate constant for
radiationless decay in a rather straightforward manner [*].
The assumptions about $u_n(\vec{r})$ are:

(i) only <u>one</u> basis function $u_0(\vec{r})$ has oscillator strength,
i.e.:

$$\langle \overline{\psi}_0 / D / u_m(\vec{r}) \rangle = D_{om} \cdot \delta_{om} \tag{1.11}$$

where D is the dipole operator.

---

[*] We will here use a somewhat generalized case in which we
relax the restrictions of constant v and ε, see further on.

We will derive that in this case $\psi_1(\vec{r},0) = u_0(\vec{r})$

From (1.5) and (1.6) we know that in general:

$$\Psi_1(\vec{r},0) = \sum_k \alpha_k \cdot \psi_k \tag{1.12}$$

with $\quad \psi_k = \sum_m (a_k)_n \, u_n(\vec{r})$

The oscillator strength of ψ_k is:

$$\langle \Psi_0 | D | \psi_k \rangle = \langle \Psi_0 | D | \sum_m (a_k)_m \cdot u_m(\vec{r}) \rangle = \sum_k (a_k)_n \, D_{om} \, \delta_{on}$$
$$= (a_k)_o \cdot D_{oc} \tag{1.13}$$

So $\quad \alpha_k \sim (a_k)_o \cdot D_{oo} \tag{1.14}$

Substituting in (1.12) gives:

$$\Psi_1(\vec{r},0) \sim \sum_k (a_k)_o \, D_{oc} \sum_m (a_k)_n \, u_m(\vec{r})$$

$$= D_{oo} \sum_k \left\{ (a_k)_o^2 \, u_o(\vec{r}) + \sum_{m \neq o} (a_k)_o \cdot (a_k)_n \, u_m(\vec{r}) \right\} \tag{1.15}$$

$$= D_{oo} \sum_k (a_k)_o^2 \cdot u_o(\vec{r}) + D_{oo} \sum_{m \neq o} \left\{ \sum_k (a_k)_o \, (a_k)_n \right\} u_m(\vec{r})$$

The vectors $\underline{a}_k$ form an orthonormal set (see (1.4)), therefore the matrix A, formed by the vectors $\underline{a}_k$, is a unitary matrix; these have the property:

$$\sum_k (a_k)_i \, (a_k)_j = \delta_{ij} \rightarrow \sum_k (a_k)_o^2 = 1 \; ; \; \sum_k (a_k)_o \cdot (a_k)_n = \delta_{on} \tag{1.16}$$

Substituting in(1.15) gives:

$$\Psi_1(\vec{r},0) \sim D_{oc} \, u_o(\vec{r}) \tag{1.17}$$

If $\psi_1(\vec{r},0)$ and $u_0(\vec{r})$ are normalized to unity, then it follows from (1.17) that $\psi_1(\vec{r},0) = u_0(\vec{r})$ q.e.d.

(ii) Further assumptions are made concerning H_{mn} in equation (1.3):

$$\begin{cases} (E_0' - E)\, a_0 \quad + \quad \sum_k N_k\, a_k \quad = 0 \\ N_1\, a_0 \quad\quad + \quad (E_1' - E)\cdot a_1 \quad = 0 \\ \vdots \qquad\qquad\qquad \vdots \\ N_k \cdot a_0 \quad\quad + \quad (E_k' - E)\cdot a_k \quad = 0 \\ \vdots \end{cases} \qquad (1.18)$$

where $E_k' = H_{kk}$; $H_{0k} = H_{k0} = v_k$ for $k > 0$.
So it is supposed that $H_{kl} = 0$ or $0 \neq k \neq l \neq 0$. Further
we call $E_k' - E_{k-1}' = \varepsilon_k$

We will only consider sets $u_n(\vec{r})$ that can be generated in a
certain way:

$$u_n(\vec{r}) = \phi_n \cdot \chi_n \cdot \qquad (1.19)$$

The functions ϕ_n and χ_n are determined by splitting the
Hamiltonian:

$$H = H_0 + T_N + H_{rest} \qquad (1.20)$$

where T_N kinetic energy operator for the nuclei.
The functions ϕ_n and χ_n further have to fulfill the eigen-
value equations:

$$(H_0 - \mathcal{E}_n)\cdot \phi_n = 0 \qquad (1.21)$$

$$(T_N + U_n - E)\, \chi_n = 0$$

with $U_n = \mathcal{E}_n + \langle \phi_n | H_{rest} | \phi_n \rangle + \langle \phi_n | T_N | \phi_n \rangle$, where the integra-
tion is over those coordinates on which χ_n does not depend.
Different sets $u_n(\vec{r})$ are then obtained by varying H_0 and
H_{rest}. Possibilities are for instance (in the following Q
and M represent the complete sets of nuclear coordinates

and masses, respectively; q denotes the complete set of electron coordinates):

(i) $H_{rest} = 0$: Adiabatic Born-Oppenheimer approximation (ABO set)

$$\mu_m(q,Q) = \phi_m(q,Q) \cdot \chi_m(Q)$$

with $\{T_E + U(q,Q) - \mathcal{E}_m(Q)\} \phi_m(q,Q) = 0$,   (1.22)

$$\{T_N + \mathcal{E}_m(Q) + (1/2M)\langle \phi_m(q,Q)|P^2|\phi_m(q,Q)\rangle_q - E\} \chi_m(Q)$$

T_E is the kinetic energy operator for the electrons, $U(q,Q)$ the Coulomb interaction between all particles and P the impulse operator for the nuclei.

(ii) $H_{rest} = U(q,Q) - U(q,Q_0)$: Crude Born-Oppenheimer approximation (CBO set)

$$\mu_m(q,Q) = \phi_m(q,Q_0) \chi_m(Q)$$

with $\{T_E + U(q,Q_0) - \mathcal{E}_m(Q_0)\} \phi_m(q,Q_0) = 0$,   (1.23)

$$\{T_N + \mathcal{E}_m(Q_0) + \langle \phi_m(q,Q_0)|U(q,Q) - U(q,Q_0)|\phi_m(q,Q_0)\rangle_q +$$

$$- E\} \cdot \chi_m(Q) = 0$$

where Q_0 is the equilibrium configuration for the nuclei.

(iii) $H_{rest} = H_{so}$, where H_{so} is the spin-orbit Hamiltonian.

(iv) $H_{rest} = U(q,Q) - U(q,Q_0) + H_{so}$

For case (iii) and (iv) the eigenvalue equations are readily derived.

1.3. Determining the Basis Set

In this chapter we will derive what portion of the eigenvalue spectrum of H is described correctly by the set $u_n(\vec{r})$, if this set satisfies the conditions (1.11) and (1.18) imposed by the generalized model of Bixon and Jortner[2], with the restriction that we will only consider sets $u_n(\vec{r})$ that can be generated with equations (1.19) to (1.21). In order to do this we will first consider the exact eigenfunctions of H, described with equations strongly reminiscent of equations (1.19) to (1.21). We will then derive under what conditions these equations simplify to the equations (1.18). We will then see that these conditions in fact constitute a limitation on the energy E for which the equations (1.18) are valid.

Generalizing the treatment of Born[4] we can write the exact eigenfunctions of H as

$$\psi = \sum_i u_i(\vec{r}) = \sum_i \phi_i \chi_i \qquad (1.24)$$

Further we write:

$$H = H_o + T_N + H_{rest} \qquad (\text{Born took } H_{rest} = 0) \qquad (1.25)$$

$$(H_o - \Phi_i)\,\phi_i = 0 \quad , \quad \Phi_i = eigenvalue$$

Now we can derive:

$$(T_N + U_i - E)\chi_i + \sum_{j \neq i} C_{ij} \cdot \chi_j = 0 \quad , \quad i = 0, 1, 2, \cdots$$

with

$$U_i = \Phi_i + \langle \phi_i | H_{rest} | \phi_i \rangle + \langle \phi_i | P^2/2M | \phi_i \rangle \qquad (1.26)$$

$$C_{ij} = \langle \phi_i | H_{rest} | \phi_j \rangle + \langle \phi_i | P^2/2M | \phi_j \rangle + \langle \phi_i | P/M | \phi_j \rangle\, P$$

Possibilities for H_{rest} are for instance:

(a) 0

(b) $U(q,Q) - U(q,Q_0)$

(c) $U(q,Q) - U(q,Q_0) + H_{so}$

(d) H_{so}

where H_{so} is the spin-orbit coupling Hamiltonian.
If possibilities (b) and (c) are used, H_0 will contain the
potential energy function $U(q,Q_0)$
By deleting the terms with the C_{ij}'s ($i \neq j$) we arrive at the
ABO's and CBO's, if we take for H_{rest} case (a) and (b),
respectively.
Now we make the expansion: $\chi_i = \sum_k a_{ik} \cdot \chi_{ik}$ with

$$(T_N + U_i - E_{ik}) \cdot \chi_{ik} = 0 \qquad (1.27)$$

where E_{ik} is the eigenvalue. Then eqs. (1.26) become:

$$(T_N + U_i - E) \sum_k a_{ik} \chi_{ik} + \sum_{j \neq i} [C_{ij} \sum_k a_{jk} \chi_{jk}] = 0, \quad i = 0,1,2.$$

from which

$$\sum_k (E_{ik} - E) a_{ik} \chi_{ik} + \sum_{j \neq i} [C_{ij} \sum_k a_{jk} \chi_{jk}] = 0.$$
$$i = 0,1,2,$$

Multiplying with χ_{ip}^{*} and integrating gives:

$$\begin{cases} (E_{op} - E) a_{op} + \sum_k a_{1k} \langle \chi_{op} | C_{01} | \chi_{1k} \rangle + \sum_k a_{2k} \langle \chi_{op} | C_{02} | \chi_{2k} \rangle + \cdots = 0, \\ \qquad\qquad\qquad\qquad\qquad\qquad\qquad\qquad\qquad\qquad\qquad p = 0,1,2, \quad (1.28) \\ (E_{1p} - E) a_{1p} + \sum_k a_{ok} \langle \chi_{1p} | C_{10} | \chi_{ok} \rangle + \sum_k a_{2k} \langle \chi_{1p} | C_{12} | \chi_{2k} \rangle + \cdots = 0, \\ \qquad\qquad\qquad\qquad\qquad\qquad\qquad\qquad\qquad\qquad\qquad p = 0,1,2, \\ (E_{2p} - E) a_{2p} + \sum_k a_{ok} \langle \chi_{2p} | C_{20} | \chi_{ok} \rangle + \cdots = 0 \quad, \quad p = 0,1,2, \\ \vdots \end{cases}$$

We will now simplify these equations until we arrive at the
set of equations (1.18). We will then see which assumptions
are implicit in the simplified equations (1.18) and whether
they are justified or not. We will look at the eigenvalues
of these equations in a certain region of E centered on E_{11};

the choice of E_{11} is arbitrary.

If (Condition I):

$$|E_{ip} - E| \gg \sum_{j \neq i} \sum_{k} a_{jk} \langle \chi_{ip} | C_{ij} | \chi_{jk} \rangle, \text{ for } i=2,3 \ldots \atop p=0,1,2,$$

then the $a_{ip} \simeq 0 (i=2,3,\ldots;p=0,1,2,\ldots)$ and eqs. (1.28) simplify to:

$$\begin{cases} (E_{op} - E) a_{op} + \sum_{k} a_{1k} \langle \chi_{op} | C_{o1} | \chi_{1k} \rangle = 0 \;,\; p = 0,1,2, \cdots \\ (E_{1p} - E) a_{1p} + \sum_{k} a_{ok} \langle \chi_{1p} | C_{10} | \chi_{ok} \rangle = 0 \;,\; p = 0,1,2, \cdots \end{cases} \quad (1.29)$$

If also (Condition II):

$$|E_{1p} - E| \gg \sum_{k} a_{ok} \langle \chi_{1p} | C_{1p} | \chi_{ok} \rangle, \text{ for } p=0,2,3 \ldots$$

then the $a_{1p} \simeq 0$ for $p = 0,2,3,\ldots$ and eqs. (1.29) simplify to:

$$\begin{cases} (E_{op} - E) a_{op} + a_{11} \langle \chi_{op} | C_{o1} | \chi_{11} \rangle = 0 \;,\; p = 0,1,2, \\ (E_{11} - E) a_{11} + \sum_{k} a_{ok} \langle \chi_{11} | C_{10} | \chi_{ok} \rangle = 0 \end{cases} \quad (1.30)$$

We have thus derived that the set (1.26) of coupled differential equations that are satisfied by the functions that determine the exact wave function, reduces to the set (1.30) of coupled linear equations for the interval S of E-values for which conditions I and II are satisfied. If we call $\langle \chi_{11} | C_{10} | \chi_{0k} \rangle = v_{k'}$ eqs. (1.30) are identical to eqs. (1.18). (Also only the state $\phi_1 \chi_{11}$ should carry oscillator strength from the ground state). This means that the space spanned by the eigenfunctions of H whose eigenvalues lie in S, is also spanned by the subset u_n that corresponds to eqs. (1.18) (while the vibrational part of u_n satisfies eq. (1.27)). This is what we set out to prove. Now we will find out what the interval S of E-values is, *i.e.* we will find those E-values for which conditions I and II are satisfied.

First we will assume that condition I is satisfied and con-
sider condition II; condition I is taken up after that.
We will estimate $\sum_k v_k \cdot a_{0k}$. If the v_k do not vary too much, we
can write $\sum_k v_k \cdot a_{0k} = v \cdot \sum_k a_{0k}$, $v =$ some average of the v_k's .

We take for the a_{0k} the ones obtained upon solving the de-
coupled eqs. (1.30); this can be considered as a zeroth
order solution for the coupled set of equations (1.29).
We obtain (see Appendix 1):

$$\left| v \sum_k a_{ok} \right| = \left| \frac{(E_{11} - E) v}{\sqrt{(E_{11} - E)^2 + (\pi v^2/\epsilon)^2}} \right| = \left| f(E) \right| \qquad (1.31)$$

with $E_{0p} - E_{0p-1} = \epsilon$ some average for all p.

To check condition II we have to compare $|f(E)|$ with $E_{12} - E$
and $E_{10} - E$; if condition II is satisfied for p=0 and p=2
for an interval of E-values, then it will be satisfied for
all $p \neq 1$ in this interval.

This is because $(E_{1p} - E) > (E_{12} - E)$, p=3,4,... (See Fig. 1.1
for the illustration of the case of p=3). Also we see that
if $(E_{12} - E) \gg v$, then $(E_{12} - E) \gg |f(E)|$.
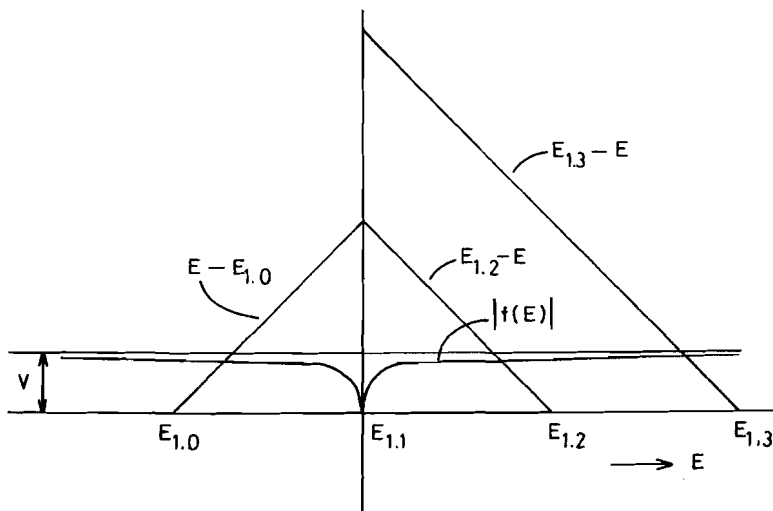
Fig. 1.1. The functions f(E), $E_{12} - E$, $E - E_{12}$ and $E_{13} - E$

Condition II is satisfied for a certain energy interval E
around E_{11}. We define a new variable Γ: $E = E_{11} + \Gamma$
Then $(E_{12}-E) >> v$ becomes

$$E_{12} - E_{11} \gg \Gamma + \mathcal{N} \rightarrow \Gamma \ll \Delta E - \mathcal{N}, \text{ with } \Delta E = E_{12} - E_{11} \qquad (1.32)$$

The maximal Γ for which this condition is satisfied is
Γ_{max}; $2\Gamma_{max}$ is the width of the E-interval around E_{11}, for
which condition II is satisfied. So:

$$\Gamma_{max} \ll \Delta E - \mathcal{N} \qquad (1.33)$$

This means that eqs. (1.30) have eigenvectors that are also
eigenvectors of H in the denoted E-interval. So we can
describe experiments in which the frequency range is less
or equal $2\Gamma_{max}$ around E_{11}.
Each eigenstate has a certain oscillator strength. The ra-
diationless decay depends on the "oscillator-profile" and
on the part of it that is excited. If we call the half-line
width of the exciting radiation Γ_b, then we can describe
the experiment if $\Gamma_{max} > \Gamma_b$.
In the model of Bixon and Jortner one derives the rate of
radiationless decay under the assumption that the whole
oscillator-profile is excited and that the oscillator-pro-
file is Lorenzian in form; this last assumption is equiva-
lent to assuming that only one zero-order state has oscilla-
tor-strength[2] and that v and ε are constants. We call the
half-line width of the oscillator-profile Γ_{op}. The whole
oscillator-profile is excited, so the whole oscillator-
profile must be described correctly with the set u_n, i.e.:

$$\left. \begin{array}{c} \Gamma_{max} \gg \Gamma_{op} \\ (1.33) \rightarrow \quad \Gamma_{max} \ll \Delta E - \mathcal{N} \end{array} \right\} \rightarrow \Gamma_{op} \ll \Delta E - \mathcal{N} \qquad (1.34)$$

If we calculate Γ_{op} with the Bixon-Jortner theory, we ob-
tain[2]:

$$\Gamma_{op} = \pi \Gamma_1 + \frac{\pi \mathcal{N}^2}{\varepsilon} + \mathcal{N}$$

Γ_1 is the half-line width of the state $\phi_1\chi_{11}$ caused by coupling with the electromagnetic field (natural line-width); v and ϵ see eq. (1.31). So we obtain:

$$\Delta E \gg \pi \Gamma_1 + \frac{\pi v^2}{\epsilon} + 2N \qquad (1.35)$$

We remark that in the whole derivation the spin state of the wave function is not specified, so the derivation is valid for both internal conversion and intersystem crossing.

Concerning condition I, we consider the case that this condition is not satisfied. The eigenvectors resulting from (1.29) and (1.30) can then be different from the exact eigenvectors with respect to eigenvalue and oscillator-strength; these two quantities determine the radiationless decay process. The eigenvalue will be higher than the eigenvalue of the corresponding exact state. The oscillator-strength can be higher or lower, so it is impossible to predict whether the radiationless decay predicted with the deficient basis set is higher or lower than the decay obtained from the exact set.

It is obvious that if one has to choose between basis sets, one will choose the one for which condition I is satisfied best[*]. It is of course possible that there is no basis set for which condition I is satisfied, $i.e.$ if there are electronic states that lie close to the excited state of interest. Under those circumstances one will have to take explicit account of the couplings with the other electronic states like in eqs. (1.29).

---

[*] See also § 2.1.1.

2. CALCULATION OF INTERNAL CONVERSION, THE METHOD

2.1. The Coupling Element

2.1.1. The Electronic Part

A. The ABO Set

From eq. (1.30) we see that the total coupling element is:

$$\langle \chi_{1p}(Q) \, | \, C_{10}(Q) \, | \, \chi_{0\ell}(Q) \rangle_Q \qquad (2.1)$$

C_{10} is the electronic coupling element. In (1.26) it is defined as:

$$C_{10} = \langle \phi_1(\ell, Q) \, | \, H_{rest} \, | \, \phi_0(q, Q) \rangle_q + \langle \phi_1(q, Q) \, | \, \frac{P^2}{2M} \, | \, \phi_0(q, Q) \rangle_q + \\ + \langle \phi_1(q, Q) \, | \, \frac{P}{M} \, | \, \phi_0(q, Q) \rangle \cdot P \qquad (2.2)$$

For the ABO set $H_{rest} = 0$, so we obtain:

$$C_{10} = \langle \phi_1(q, Q) \, | \, \frac{P^2}{2M} \, | \, \phi_0(q, Q) \rangle_q + \langle \phi_1(q, Q) \, | \, \frac{P}{M} \, | \, \phi_0(q, Q) \rangle_q \cdot P \qquad (2.3)$$

The impulse operator P can be expressed in mass-weighted normal coordinates Q_k: (Q stands for Q_1, Q_2,..., Q_N, N = the number of normal coordinates)

$$C_{10} = -\frac{1}{2} \sum_k \langle \phi_1(q, Q) \, | \, \frac{\partial^2}{\partial Q_k^2} \, | \, \phi_0(q, Q) \rangle_q - \sum_k \langle \phi_1(q, Q) \, | \, \frac{\partial}{\partial Q_k} \, | \, \phi_0(q, Q) \rangle_q \cdot \frac{\partial}{\partial Q_k} \qquad (2.4)$$

Generally the first term is considered smaller than the second one. The first term can be expanded as (Appendix 2):

$$\langle \phi_1 \, | \, \frac{\partial^2}{\partial Q_k^2} \, | \, \phi_0 \rangle_q = \sum_p \langle \phi_1 \, | \, \frac{\partial}{\partial Q_k} \, | \, \phi_p \rangle_q \langle \phi_p \, | \, \frac{\partial}{\partial Q_k} \, | \, \phi_0 \rangle_q + \frac{\partial}{\partial Q_k} \langle \phi_1 \, | \, \frac{\partial}{\partial Q_k} \, | \, \phi_0 \rangle_q \qquad (2.5)$$

The summation p is over all electronic states different from 0 and 1. The first term in this expression is small if condition I is satisfied. If we also assume that $<\phi_1|\frac{\partial}{\partial Q_k}|\phi_0>_q$ varies only slowly with Q_k, then the second term in (2.5) will also be small.

It would be interesting to calculate this coupling, because it gives information on how well condition I is satisfied. The calculation leads, however, to very many rather complicated integrals (see Appendix 3) and has therefore not been undertaken in the present work.

So, C_{10} reduces to:

$$C_{10} = -\sum_k <\phi_1(q,Q)|\frac{\partial}{\partial Q_k}|\phi_0(q,Q)>_q \frac{\partial}{\partial Q_k} \qquad (2.6)$$

$$= -\sum_k \frac{<\phi_1(q,Q)|\frac{\partial U(q,Q)}{\partial Q_k}|\phi_0(q,Q)>}{\mathcal{E}_0(Q) - \mathcal{E}_1(Q)} \frac{\partial}{\partial Q_k} \qquad \begin{array}{l}(see \\ App.4)\end{array} \quad (2.7)$$

U represents all potential energy terms: electron-electron repulsion, nuclear-nuclear repulsion and electron-nuclear attraction.

The first term does not contribute, because it doesn't depend on Q_k ; the second term does not contribute because it doesn't depend on q, which causes the integral over q to be zero, because ϕ_0 and ϕ_1 are orthogonal.

This leaves $\qquad \frac{\partial U(q,Q)}{\partial Q_k} = \frac{\partial}{\partial Q_k} V_{en} = \frac{\partial}{\partial Q_k} \left\{ -\sum_e \sum_n \frac{z_n}{r_{en}} \right\} \qquad (2.8)$

The summations e and n are over all electrons and nuclei, respectively. z_m is the nuclear charge and r_{en} is the electron-nucleus distance:

$$r_{en} = \left\{ \sum_{j=1}^{3} (s_j^m - e_j^i)^2 \right\}^{\frac{1}{2}} , \quad j = x,y,z. \qquad (2.9)$$

23

s_j^n and q_j^e are the Cartesian coordinates of nucleus and electron, respectively.

In order to differentiate r_{en} we will first transform $\dfrac{\partial}{\partial Q_k}$:

$$\frac{\partial}{\partial Q_k} = \sum_{n'} \sum_{j'} \left\{ \frac{\partial s_{j'}^{n'}}{\partial Q_k} \right\} \frac{\partial}{\partial s_{j'}^{n'}} \quad , \; j' = x, y, z \; ; \; n' \text{ runs over all nuclei.} \tag{2.10}$$

The differential quotients $\left\{ \dfrac{\partial s_{n'}^{j'}}{\partial Q_k} \right\}$ are the elements $D_{j'k}^{n'}$ of the Jacobian matrix D that transforms normal coordinates to Cartesian coordinates. This matrix can be determined from a normal coordinate analysis (see Chapter 2.4.). From eq. (2.8) and eq. (2.10) it follows that:

$$\frac{\partial}{\partial Q_k} V_{en} = \sum_{n'} \sum_{j'} D_{j'k}^{n'} \frac{\partial}{\partial s_{j'}^{n'}} \left\{ - \sum_{e} \sum_{n} \frac{z_n}{r_{en}} \right\} \tag{2.11}$$

r_{en} depends only on the coordinates of one nucleus n , so:

$$\frac{\partial}{\partial Q_k} V_{en} = \sum_{n} \sum_{j'} D_{j'k}^{n} \sum_{e} \left\{ - \frac{\partial}{\partial s_{j'}^{n}} \frac{z_n}{r_{en}} \right\} \tag{2.12}$$

From eq. (2.9) it follows that:

$$\frac{\partial}{\partial s_{j'}^{n}} \left(r_{en}^{-1} \right) = \frac{- (s_{j'}^{n} - q_{j'}^{e})}{r_{en}^3} \tag{2.13}$$

Now we obtain:

$$\left\langle \phi_1 (q, Q) \left| \frac{\partial u}{\partial Q_k} \right| \phi_2 (q, Q) \right\rangle_q =$$

$$= \sum_{n} \sum_{j'} D_{j'k}^{n} \, z_n \left\langle \phi_1 (q, Q) \left| \frac{\sum_{e} - (q_{j'}^{e} - s_{j'}^{n})}{r_{en}^3} \right| \phi_2 (q, Q) \right\rangle_q \tag{2.14}$$

Now is $\sum_{e} \dfrac{q_{j'}^{e} - s_{j'}^{n}}{r_{en}^3}$ the j'th component of the electric field opera- tor for nucleus n.

We call the vector

$$\left\langle \phi_1(q,Q) \left| \frac{\sum_i (q_i^2 - S_{ji}^n)}{r_{in}^3} \right| \phi_o(q,Q) \right\rangle_q = \vec{E}_{jn}^{\prime\prime 0}(Q) \tag{2.15}$$

We define a new index p; p runs over the Cartesian compo-
nents of all the nuclei; Z_p then equals the charge of nu-
cleus 1 for p = 1,2,3, similarly for the other nuclei.
Eq. (2.14) then becomes:

$$\left\langle \phi_1(q,Q) \left| \frac{\partial U}{\partial Q_k} \right| \phi_o(q,Q) \right\rangle_q = -\sum_p D_{kp} \cdot Z_p \cdot E_p^{\prime\prime 0}(Q) = V_k^{\prime\prime 0}(Q) \tag{2.16}$$

So C_{10} becomes (see 2.7):

$$C_{10}'(Q) = \sum_k \frac{V_k^{\prime\prime 0}(Q)}{\mathcal{E}_o(Q) - \mathcal{E}_1(Q)} \cdot \frac{\partial}{\partial Q_k} \tag{2.17}$$

B. The CBO set

From eq. (2.2):

$$C_{10} = \left\langle \phi_1(q,Q_o) | H_{rest} | \phi_o(q,Q_o) \right\rangle_q + \left\langle \phi_1(q,Q_o) \left| \frac{P^2}{2M} \right| \phi_o(q,Q_o) \right\rangle_q + \tag{2.18}$$
$$+ \left\langle \phi_1(q,Q_o) \left| \frac{P}{M} \right| \phi_o(q,Q_o) \right\rangle_q \cdot P$$

$$H_{rest} = U(q,Q) - U(q,Q_o) \tag{2.19}$$

So:

$$C_{10} = \left\langle \phi_1(q,Q_o) | U(q,Q) - U(q,Q_o) | \phi_o(q,Q_o) \right\rangle_q \tag{2.20}$$

$$U = V_{ee} + V_{en} + V_{nn} \tag{2.21}$$

The V_{nn} will not contribute, because it does not depend on
q (ϕ_1 and ϕ_0 are orthogonal).

$$U(q,Q) - U(q,Q_o) = V_{en}(q,Q) + V_{ee} - \left(V_{en}(q,Q_o) + V_{ee} \right) = V_{en}(q,Q) - V_{en}(q,Q_o) \tag{2.22}$$

So we obtain:

$$C_{10} = \langle \phi_1(q,Q_o) | V_{en}(q,Q) - V_{en}(q,Q_o) | \phi_o(q,Q_o) \rangle_q \qquad (2.23)$$

$$\text{With} \quad V_{en} = \sum_{e} \sum_{n} \frac{-z_n}{r_{en}} \text{ , summing over electrons and nuclei.} \qquad (2.24)$$

Now is $\sum_{e} \frac{1}{r_{en}}$ the potential energy operator for the inter-action between nucleus n and all electrons.

We call

$$\langle \phi_1(q,Q_o) | \sum_{e} \frac{1}{r_{en}} | \phi_o(q,Q_o) \rangle_q = {}^{c}V_n^{10}(Q) \qquad (2.25)$$

So eq. (2.23) becomes

$$C_{10}(Q) = \sum_{n} z_n \left\{ {}^{c}V_n^{10}(Q) - {}^{c}V_n^{10}(Q_o) \right\} \qquad (2.26)$$

2.1.2. The Vibrational Part

A. The ABO Set

The total coupling element is (2.1):

$$\langle \chi_{1p}(Q) | C_{10}(Q) | \chi_{oq}(Q) \rangle_Q \text{ , using eq. (2.17) we obtain} \qquad (2.27)$$

$$\langle \chi_{1p}(Q) | \frac{\sum_{k} V_k^{10}(Q) \frac{\partial}{\partial Q_k}}{\mathcal{E}_1(Q) - \mathcal{E}_o(Q)} | \chi_{oq}(Q) \rangle_Q \qquad (2.28)$$

The χ are solutions of (1.22):

$$\left\{ T_N + \mathcal{E}_i(Q) + \langle \phi_i(q,Q) | \frac{P^2}{2M} | \phi_i(q,Q) \rangle_q - E_{im} \right\} \chi_{im}(Q) = 0 \qquad (2.29)$$

(Q and M represent the complete sets of nuclear coordinates and masses, respectively).

We neglect $\frac{1}{2M} \langle \phi_i(q,Q)|P^2|\phi_i(q,Q)\rangle_q$ because the $\frac{1}{2M}$ factor will make this term small compared to the other terms. We can let Q now represent the complete set of normal coordinates:

$$\{ T_N + \bar{\Phi}_i(Q) - \mathcal{E}_{im} \} \chi_{im}(Q) = 0 \qquad (2.30)$$

If $\bar{\Phi}_i(Q) = \bar{\phi}_i(Q_0) + \sum_k \bar{\phi}_i(Q_k)$ *) then $\qquad (2.31)$

$$\chi_{im}(Q) = \prod_k \chi_{im}(Q_k) \text{ with } \{ T_N + \bar{\phi}_i(Q_k) - \mathcal{E}_{in}^k \} \chi_{in}(Q_k) = 0 \qquad (2.32)$$

$$\text{and } \mathcal{E}_{im} = \bar{\phi}_i(Q_0) + \sum_k \mathcal{E}_{im}^k \qquad (2.33)$$

Then the coupling element becomes:

$$\sum_m \prod_k \langle \chi_{ip}(Q_k)| \frac{V_m'^0(Q)}{\bar{\phi}_i(Q) - \bar{\phi}_0(Q)} \frac{\partial}{\partial Q_m} | \prod_\ell \chi_{oq}(Q_\ell) \rangle_Q \qquad (2.34)$$

We assume that:

$$\frac{V_m''^0(Q)}{\bar{\phi}_i(Q) - \bar{\phi}_i(Q)} = V_{mE}''^0(Q) = V_{mE}''^0(Q_0) + \sum_\ell V_{nE}''^0(Q_\ell) \qquad (2.35)$$

Substituting (2.35) in (2.34) we obtain:

$$\sum_m V_{mE}''^0(Q_0) \cdot \prod_{k \neq m} \langle \chi_{ip}(Q_k)|\chi_{oq}(Q_k)\rangle \langle \chi_{ip}(Q_m)|\frac{\partial}{\partial Q_m}|\chi_{oq}(Q_m)\rangle +$$

$$+ \sum_m \sum_\ell \prod_{\substack{k \neq m \\ \neq \ell}} \langle \chi_{ip}(Q_\ell)| V_{mE}''^0(Q_\ell) \cdot \{ 1 - \delta_{\ell m}(1 - \frac{\partial}{\partial Q_\ell}) \} |\chi_{oq}(Q_\ell)\rangle * \qquad (2.36)$$

$$* \Big[\langle \chi_{ip}(Q_m)|\frac{\partial}{\partial Q_m}|\chi_{oq}(Q_m)\rangle \cdot (1 - \delta_{\ell m}) + \delta_{\ell m} \Big] \cdot \langle \chi_{ip}(Q_k)|\chi_{oq}(Q_k)\rangle$$

---

*) It is observed that we take the same normal coordinates for both ground and excited state, *i.e.*: we neglect the so-called Duschinsky effect[8].

This is the total expression for the coupling. There occur
4 different types of integrals in this expression.

B. The CBO Set

The total coupling element is (2.1):

$$\langle \chi_{ip}(Q) \,|\, C_{io}(Q) \,|\, \chi_{of}(Q) \rangle_{Q} \tag{2.37}$$

with $\quad C_{io}(Q) = \sum_{m} z_{m}\{{}^{c}V_{m}^{io}(Q) - {}^{c}V_{m}^{io}(Q_{o})\} \qquad$ (see (2.26))

The χ are solutions of:

$$\{T_{N} + \bar{E}_{i}(Q_{o}) + \langle \phi_{i}(q \cdot Q_{o})\,|\,U(q,Q) - U(q,Q_{o})\,|\,\phi_{i}(q,Q_{o})\rangle_{q} - E_{in}\}\chi_{in}(Q) = 0 \tag{2.38}$$

If we assume that:

$$\langle \phi_{i}(q\,Q_{o})\,|\,U(q,Q)\,|\,\phi_{i}(q,Q_{o})\rangle_{q} = \sum_{k} \langle \phi_{i}(q,Q_{o})\,|\,U(q,Q_{k})\,|\,\phi_{i}(q,Q_{o})\rangle_{q} \tag{2.39}$$

with Q_{k} the normal coordinates, then:

$$\chi_{in}(Q) = \overline{\prod_{k}} \chi_{in}(Q_{k}) \tag{2.40}$$

The coupling element becomes:

$$\prod_{k}\prod_{l} \langle \chi_{ip}(Q_{k})\,|\,C_{io}(Q)\,|\,\chi_{of}(Q_{l})\rangle \tag{2.41}$$

If we assume that $\qquad C_{io}(Q) = C_{io}(Q_{o}) + \sum_{m} C_{io}(Q_{m})$

then (2.41) becomes

$$\sum_{m}\prod_{k}\prod_{l} \langle \chi_{ip}(Q_{k})\,|\,C_{io}(Q_{m})\,|\,\chi_{of}(Q_{l})\rangle_{Q}$$

$$= C_{io}(Q_{o})\cdot\prod_{k}\langle \chi_{ip}(Q_{k})\,|\,\chi_{of}(Q_{k})\rangle + \sum_{m}\prod_{k}\langle \chi_{ip}(Q_{k})\,|\,C_{io}(Q_{m})\,|\,\chi_{of}(Q_{k})\rangle \tag{2.42}$$

$$= C_{io}(Q_{o})\cdot\prod_{k}\langle \chi_{ip}(Q_{k})\,|\,\chi_{of}(Q_{k})\rangle + \sum_{m}\prod_{k \neq m}\langle \chi_{ip}(Q_{m})\,|\,C_{io}(Q_{m})\,|\,\chi_{of}(Q_{m})\rangle \ast$$

$$\ast \langle \chi_{ip}(Q_{k})\,|\,\chi_{of}(Q_{k})\rangle$$

2.2. The Rate of Radiationless Decay

Radiationless decay is described by the decrease of oscillator-strength due to interference of eigenstates of the Hamiltonian. (The total rate of decay also includes decay of the initial state *via* other processes).
So we first have to know the eigenvectors of H. We simply determine the exact eigenvectors by diagonalizing the interaction matrix H_{mn} (see (1.5)). The matrix H will have the form

$$
\begin{pmatrix}
E_0' & \nu_1 & \nu_2 & \nu_3 & . & \cdot \\
\nu_1 & E_1' & & & \bigcirc \\
\nu_2 & & E_2' & \\
\nu_3 & & & E_3' & \cdot \\
\vdots & \bigcirc & & & \cdot \cdot
\end{pmatrix}
\tag{2.43}
$$

in which $E_k' = \langle \mu_k | H | \mu_k \rangle$ and $\nu_k = H_{ok} = \langle \mu_o | H | \mu_k \rangle$ (compare (1.18))

with $\quad \mu_0 = \phi_1 \chi_{11}$ (excited state)

$\quad\quad \mu_k = \phi_c \chi_{ok}$ (high vibrational level of ground state)

To be exact we have to add complex terms to the elements of the interaction matrix [3,4,5,6] to describe decay of the zero-order states *via* other processes. The most well-known of these is the decay by fluorescence. However, this can be treated as an independent decay channel[1], if the irradiation time is short compared to the radiative lifetime, *i.e.* in the short time experiment, which is the case that we are considering.
The resulting eigenvectors are $\underline{a}_k = \begin{pmatrix} (a_k)_o \\ (a_k)_1 \\ \vdots \end{pmatrix}$ with eigenvalue E_k.

We are interested in the oscillator strength of ψ_1: (see (1.9)).

$$f \sim \left| \left< \bar{\Psi}_o \middle| D \middle| \bar{\Psi}_1 \right> \right|^2 \tag{2.44}$$

If only u_0 has oscillator-strength with ψ_0, then this formula reduces to

$$f \sim \left| \left< \bar{\Psi}_o \middle| D \middle| \sum_k \alpha_k \, (a_k)_o \, e^{-i E_k t} \cdot u_o \right> \right|^2 \tag{2.45}$$

We know that, if only u_0 has oscillator-strength, then $\alpha_k \sim (a_k)_0$ (see(1.14)). So we obtain:

$$f \sim \left| \left< \bar{\Psi}_o \middle| D \middle| u_o \right> \sum_k (a_k)_o^2 \, e^{-i E_k t} \right|^2$$

$$= \left| \sum_k (a_k)_o^2 \, e^{-i E_k t} \right|^2 \tag{2.46}$$

$$= P_1 (t)$$

If $\log P_1(t)$ *versus* t gives a straight line, then we have exponential decay. However, we can also detect deviations from exponential decay with this method. The diagonalizing and summing are programmed in the INTERF program.
If all v_i are equal, and $E_k' - E_{k-1}' = \varepsilon$ = constant (the original Bixon-Jortner model) then we can obtain eigenvectors of H_{mn} in an analytical way.
For $P_1(t)$ we obtain:

$$P_1(t) = e^{-\left(\frac{\pi v^2}{\varepsilon} + w \right) \cdot t} \tag{2.47}$$

2.3. Normal Coordinates

In paragraph 2.2. it turned out that we need the normal coordinates of the molecule concerned; we also need the matrix D that transforms normal coordinates to Cartesian coordinates (formula 2.10).

We shall denote the main features of the derivation of these quantities[9],[10].

In Classical Mechanics the equations of motion are the Lagrange equations:

$$\frac{d}{dt}\left(\frac{\partial T}{\partial \dot{r}_i}\right) + \frac{\partial V}{\partial r_i} = 0 \quad , \quad i = 1,2,\cdots \qquad (2.48)$$

T is the kinetic energy, V is the potential energy, r_i is the space coordinate, $\dot{r}_i = \frac{\partial r_i}{\partial t}$, t is the time. In Cartesian coordi-   nates they take the form:

$$\frac{1}{m_i}\frac{\partial^2}{\partial t^2} x_i + \sum_{j=1}^{3N} f_{ij} \, x_i = 0 \quad , \quad i = 1,2,\cdots,3N \qquad (2.49)$$

m_i is the mass of particle i, N is the number of particles, x_i is a Cartesian coordinate.

We define internal coordinates $S_t = \sum_{i=1}^{3N} B_{ti} \cdot x_i$, $t = 1,2,\cdots,3N-6$

then: $2T = \sum_{t,t'} (G^{-1})_{tt'} \dot{S}_t \dot{S}_{t'}$ with $G^{-1}_{tt'} = \sum_{i=1}^{3N} \frac{1}{m_i} B_{ti} \, B_{t'i}$ (2.50)

and $2V = \sum_{t,t'} F_{tt'} \cdot S_t \, S_{t'}$ with $F_{tt'} = \sum_{i,j} B_{ti} \, f_{ij} \, B_{jt'}$

and the equations of motion become:

$$\sum_{j}\left\{ F_{ij} + (G^{-1})_{ij} \cdot \frac{\partial^2}{\partial t^2} \right\} S_j = 0 \quad , \quad i = 1,2,\cdots,3N-6 \qquad (2.51)$$

Making the multiple substitutions

$$S_{ik} = l_{ik} \, \cos(2\pi \nu_k t + P) \quad \text{and}$$

$$\ddot{S}_i = -\lambda_k \cdot l_{ik} \, S_i \quad \text{with} \quad \lambda_k = 4\pi^2 \nu_k^2 = \omega_k^2, \text{ for } k = 1,2,\cdots,3N-6$$

we obtain the secular equations:

$$\sum_j \left\{ F_{ij} - \lambda_k \left(g^{-1} \right)_{ij} \right\} \cdot l_{ik} = 0 \quad , \; k = 1,2, \dots , 3N-6 \qquad (2.52)$$

Multiplying on the left with G gives:

$$\sum_j \left\{ \left(g F \right)_{ij} - \lambda_k \; \delta_{ij} \right\} \cdot l_{jk} = 0 \quad , \; k = 1,2, \dots , 3N-6 \qquad (2.53)$$

Before continuing we must remark that often internal sym-
metry coordinates are used instead of internal coordinates,
because then the F and G matrix reduce to a block-diagonal
matrix, the different blocks corresponding to the different
irreducible representations. We will denote matrices and
vectors in internal symmetry coordinates with script capi-
tals (e.g. S, G, F).
We write $\quad \mathscr{S}_i = \sum_t \mathcal{U}_{it} \cdot S_t$.

If one works in internal symmetry coordinates, all capitals
in the following should be changed to script capitals.
The making of matrix U can give problems if more than one
normal coordinate belongs to the same degenerate (e.g. E)
representation. The generators - that generate the symmetry
coordinates *via* the projection operator - then must have
the same transformation properties (remain invariant under
the same operators), because otherwise the blocks to which
F reduces (in the internal symmetry coordinate representa-
tion) will not be identical for this degenerate represen-
tation; this will give difficulties if one wants to make
use of this property (manual calculations).
We return to equation (2.53). The direct calculation of the
eigenvectors L of GF is difficult because GF is not a sym-
metricl matrix, although G and F are. In practice, one
therefore takes a different matrix H, that is symmetric
and that has the same eigenvectors as GF .

L is the matrix of eigenvectors of GF , this matrix also
diagonalizes F : L'FL = Λ (L' = L$^{\text{transposed}}$), Λ is a diagonal
matrix with the eigenvalues λ_k .

If we define $\quad Q_i = \sum_j (L^{-1})_{ij} S_j \ , \quad i = 1, 2, \dots, 3N-6$

then it turns out that $\quad V = \frac{1}{2} \sum_i Q_i^2 \lambda_i \quad$ and $\quad T = \frac{1}{2} \sum_i \dot{Q}_i^2 \ ,$ so the Q_i

are the normal coordinates.

We write: $\quad Q = L^{-1} S = L^{-1} B x$.

We can also derive[9] $\quad x = M^{-1} B' (L^{-1})' Q \qquad (2.54)$

in which M^{-1} is a diagonal matrix $3N \times 3N$ with on the diagonal the inverse of the atomic mass, three times for each atom.

One can also derive $\quad x = (L^{-1} B M^{-1})' Q \qquad (2.55)$

So we need the matrix $(L^{-1} B M^{-1})^1$ to calculate the normal coordinates.

We also need this same matrix in eq. (2.10) for the matrix D because:

$$\frac{\partial x}{\partial Q} = (L^{-1} B M^{-1})' \qquad (2.56)$$

3. CALCULATION OF INTERNAL CONVERSION IN FORMALDEHYDE

3.0. The Choice of Formaldehyde

There is a number of reasons why formaldehyde was chosen as an example of the calculation of radiationless decay:

- Formaldehyde is small enough to be subject to accurate *ab initio* calculations.
- The vibrational levels of formaldehyde in the $n\pi^*$-state are sufficiently separated, so that they can be excited selectively, this in contradistinction to the aromatic hydrocarbons. The radiationless decay for a number of these levels has been measured (see 4.2.).
- The rovibronic analysis of the ground and $n\pi^*$-excited state is completely known (see 4.1.).
- Formaldehyde can also serve as a model for photodissociation, because after exciting the $n\pi^*$-state, dissociation takes place *via* a radical (H - HCO) or a molecular process $(H_2 + CO)$.
  The S_1-levels are sharp and the high S-levels are broadened to a quasi-continuum. Yeung and Moore[44,45] conclude from this that S_0 does not, but S_1 does couple with the dissociative continue, and that the rate-determining step for the dissociation is the $S_1 \rightarrow S_0$ internal conversion.

A potential difficulty is formed by the triplet state T_1, which lies 3000 cm^{-1} below the S_1 level. This means that the density of triplet levels, for energies lying in the S_1 spectrum, is only slightly greater than the density of the corresponding S_1 levels. In accordance with this, experiments have never shown phosphorescence after excitation of the S_1 state, only after direct excitation of the T_1

state[46].

Tang *et al.*[47] have also concluded that for the $2^2 4^1$ level, for which strong S-T perturbation has been observed, the triplet state must have a minor or negligible role in the photochemical mechanism for this level, with the $S_1 \rightarrow S_0$ internal conversion probably the most important pathway for its radiationless decay.

3.1. Calculation of the Normal Coordinates

The formaldehyde molecule has C_{2v} symmetry in the ground state equilibrium geometry (see Fig. 3.1.). The representation for the vibrations is: $\Gamma = 3A_1 + B_1 + 2B_2$. Therefore, the matrix F reduces as follows (see eq. (2.53) and further):

$$\begin{pmatrix} x & x & x & & & \\ x & x & x & & O & \\ x & x & x & & & \\ & & & x & & \\ & & & & x & x \\ & O & & & x & x \end{pmatrix}$$

It follows that there are 10 independent force constants in the general harmonic force field (F is also symmetric). Duncan and Mallinson[1] have determined these 10 force constants from the IR, Raman and microwave spectra of formaldehyde and its isotopes; these form the matrix F. The equilibrium geometry used by Duncan and Mallinson is shown in Fig. 3.1.
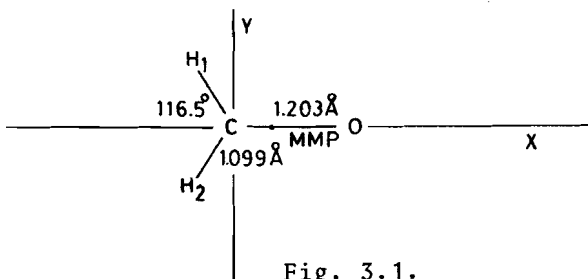
Fig. 3.1.

The internal coordinates are: r_1 and r_2, the CH_1 and CH_2 distances; R the CO distance; α the H_1CH_2 angle; β_1 and β_2 the H_1CO and H_2CO angles; γ the angle the CO bond makes with the HCH plane.
The internal symmetry coordinates are:

$$S_1 = 2^{-\frac{1}{2}}(\delta r_1 + \delta r_2) \qquad\qquad S_4 = \delta\gamma$$
$$S_2 = \delta R \qquad\qquad\qquad\qquad\quad S_5 = 2^{-\frac{1}{2}}(\delta r_1 - \delta r_2)$$
$$S_3 = 6^{-\frac{1}{2}}(2\delta\alpha - \delta\beta_1 - \delta\beta_2) \qquad S_6 = 2^{-\frac{1}{2}}(\delta\beta_1 - \delta\beta_2)$$

The nuclear masses used, are those of the $^{12}_{6}C$, $^{16}_{8}O$ and $^{1}_{1}H$ isotopes[2]. Now the B and G matrices are determined with the computer program GMOPREAL[3]. The input consists of geometry, nuclear masses, definition of internal coordinates and internal symmetry coordinates.
Then we use the program VSEC[3] to calculate L^{-1} by diagonalizing the Wilson GF vibration secular equations (eq. (2.53)). The input consists of: G , F , B = UB, the geometry and the masses. We can now calculate the matrix $(L^{-1}BM^{-1})'$ (' means transposed), by simple matrix multiplication. This is the matrix we need to calculate the cartesian coordinates of different points of the normal coordinate path:

$$x = (\mathcal{L}^{-1}\mathcal{B}\,M^{-1})'\,\mathcal{Q}$$

Also this same matrix is used in eq. (2.10).

A few words about dimensions and units.
The normal coordinates resulting from the VSEC program have the dimension $(a.w.C)^{\frac{1}{2}}$ Å = 80.9742 $(a.m.u.)^{\frac{1}{2}}$ a.l.u. = 1.889726 $(a.w.C)^{\frac{1}{2}}$ a.l.u. with: a.w.C = atomic weight scale based on C; a.m.u. = atomic mass unit; a.l.u. = atomic length unit.
The $(L^{-1}BM^{-1})'$ matrix calculated with the VSEC program converts normal coordinates to cartesian coordinates, *i.e.* $(a.w.C)^{\frac{1}{2}}$ Å to Å, and so the $(L^{-1}BM^{-1})'$ matrix elements have the dimension $(a.w.C)^{-\frac{1}{2}}$ = 0.02317 $(a.m.u.)^{-\frac{1}{2}}$.

We can also relate the normal coordinate for the out-of-plane bending to the out-of-plane angle γ.
The kinetic energy in terms of normal and internal coordinates must be the same:

$$2T = \dot{Q_4}^2 = \frac{1}{G_{44}} \cdot \dot{S_4}^2 .$$

(3.1)

so: $\quad Q_4 = \frac{1}{\sqrt{G_{44}}} S_4 = (\mathcal{L}^{-1})_{44} \cdot S_4$

(G_{44} is sometimes called the reduced mass).
Jones and Coon[41] derived that for formaldehyde one can also write:

$$2T = \dot{Q_4}^2 = \mu(\gamma) \cdot r^2 \cdot \dot{\gamma}^2 \Rightarrow dQ_4 = \mu(\gamma)^{\frac{1}{2}} \cdot r \cdot d\gamma \Rightarrow$$

$$Q_4 = \int_0^\gamma \mu(\gamma)^{\frac{1}{2}} r \, d\gamma .$$

(3.2)

with γ = the out-of-plane angle in radians
r = the CO distance in $\mathring{A}$
$\mu(\gamma)$ is the reduced mass corresponding to the internal coordinate $r\gamma$ for the out-of-plane bending:

$$\mu(\gamma) = -\frac{2M_H \cdot l \, (m + l \cdot n \cdot \sin^2\gamma)}{n(1-m) + 2 \, l \, n \, R \cos\gamma + l \, (1-l) R^2}$$

(3.3)

with $1 = \dfrac{M_O}{M}$, $\quad m = \dfrac{M_C}{M}$, $\quad n = \dfrac{2M_H}{M}$, $\quad M = M_O + M_C + 2M_H$

$R = \dfrac{r}{s \cos\beta}$, s = C-H distance, 2β = the HCH angle.

We now want to extend the usual application of normal coordinates to rotations and translations. The definition of a normal coordinate is that the potential and kinetic energy for the normal coordinate movement can be written as: $V = \lambda Q^2$ and $T = \frac{1}{2}\dot{Q}^2$, respectively. For rotations and translations V is constant, so we can set $\lambda = 0$. We only have to be concerned with the kinetic energy for these movements.
We will first treat the translations.

Translation along the x-axis corresponds with a kinetic energy of: $T = \frac{1}{2} \sum_i m_i \cdot \dot{x}_i^2$

The normal coordinate Q is defined as $T = \frac{1}{2} \dot{Q}^2$.

So $\qquad x_i = \frac{1}{\sqrt{m_T}} \, Q$

$$(3.4)$$

with $\qquad m_T = \sum_i m_i$

So $\frac{1}{\sqrt{m_T}}$ is a matrix element of the $(L^{-1}BM^{-1})'$ matrix, because this matrix transforms Q into x (see eq. (2.55)).

For the rotations we first need to know the center of mass. For formaldehyde it lies on the CO axis, between C and O, at a distance of 0.602 Å from C. The principal axes are the x-axis and the axes parallel to the y- and z-axis, going through the center of mass. Formaldehyde is an asymmetric top molecule, with three different moments of inertia I_A, I_B and I_C (in order of decreasing magnitude). But as $I_B \approx I_C$ the system behaves very much like a prolate symmetric top molecule.

The rotation around an axis parallel to the y-axis will be given as an example. First the distances of the atoms to the axis of rotation are calculated:

r_C = 0.602 A, r_O = 0.601 A, r_{H_1} = r_{H_2} = 1.180 A.

We now write down the kinetic energy, valid for a rotation over small angles:

$$T = \frac{1}{2}\left(m_O \cdot \dot{z}_O^2 + m_C \cdot \dot{z}_C^2 + m_{H_1} \cdot \dot{z}_{H_1}^2 + m_{H_2} \cdot \dot{z}_{H_2}^2 \right) \quad (3.5)$$

z_P being the vertical displacement of P.

We now express all z's in $z = z_O$:

$$z_O = z, \quad z_C = \frac{r_C}{r_O} \cdot z, \quad z_{H_1} = z_{H_2} = \frac{r_H}{r_O} \cdot z \qquad (3.6)$$

This gives: $T = \frac{1}{2}\left(m_O \cdot \dot{z}^2 + m_C \frac{r_C^2}{r_O^2} \dot{z}^2 + 2m_H \frac{r_H^2}{r_O^2} \cdot \dot{z}^2 \right) \quad (3.7)$

$$
\begin{pmatrix}
0.0586 & 0 & 0 & 0.0004 & 0 & 0 & -0.3529 & 0.5924 & 0 & -0.3529 & -0.5924 & 0 \\
-0.2141 & 0 & 0 & 0.1448 & 0 & 0 & 0.1262 & 0.2007 & 0 & 0.1262 & -0.2007 & 0 \\
0.0254 & 0 & 0 & -0.0906 & 0 & 0 & 0.5676 & 0.3237 & 0 & 0.5676 & -0.3237 & 0 \\
0 & 0 & -0.1481 & 0 & 0 & 0.0361 & 0 & 0 & 0.5958 & 0 & 0 & 0.5958 \\
0 & -0.0938 & 0 & 0 & -0.0006 & 0 & -0.3546 & 0.5636 & 0 & 0.3546 & 0.5636 & 0 \\
0 & 0.1283 & 0 & 0 & -0.0681 & 0 & -0.5576 & -0.2238 & 0 & 0.5576 & 0.2238 & 0 \\
0 & 0 & 0 & 0 & 0 & 0 & 0 & 0 & -0.7043 & 0 & 0 & 0.7043 \\
0 & 0 & -0.1672 & 0 & 0 & 0.1672 & 0 & 0 & -0.3284 & 0 & 0 & -0.3284 \\
0 & 0.1573 & 0 & 0 & -0.1573 & 0 & 0.3335 & 0.2078 & 0 & -0.3335 & 0.2078 & 0 \\
0.0333 & 0 & 0 & 0.0333 & 0 & 0 & 0.0333 & 0 & 0 & 0.0333 & 0 & 0 \\
0 & 0.0333 & 0 & 0 & 0.0333 & 0 & 0 & 0.0333 & 0 & 0 & 0.0333 & 0 \\
0 & 0 & 0.0333 & 0 & 0 & 0.0333 & 0 & 0 & 0.0333 & 0 & 0 & 0.0333
\end{pmatrix}
$$

Table 3.1. The $(L^{-1}BM^{-1})'$ matrix

If we take:

$$z = \left(m_O + m_C \cdot \frac{h_C^2}{h_O^2} + 2 m_H \cdot \frac{h_H^2}{h_O^2} \right)^{-\frac{1}{2}} \cdot \dot{Q} = 0.167 \, \dot{Q} \qquad (3.8)$$

(masses in a.w.C)

then we obtain: $T = \frac{1}{2} \dot{Q}^2$.

Having obtained z, all z_p's can be calculated from it.
For rotation around the x-axis: $r_C = r_O = 0$, $r_{H_1} = r_{H_2} = 0.9345$ Å. For rotation around the axis parallel to the z-axis: $r_C = 0.601$ Å, $r_C = 0.602$ Å, $r_{H_1} = r_{H_2} = 1.505$ Å.
The $(L^{-1}BM^{-1})'$ matrix in (a.m.C)$^{-\frac{1}{2}}$ is given in Table 3.1.
Cartesian coordinates vertically, normal coordinates horizontally; the cartesian coordinates have the order C, O, H, H; the normal coordinates have the order: vibrations, rotations, translations.

One general remark concerning the use of normal coordinates must be made. The normal coordinates we used so far are linear coordinates, because they are generated with a matrix $(L^{-1}BM^{-1})'$ with elements that are constants. This has the effect that these normal coordinates cannot describe pure bendings and rotations. For rotations it is especially obvious that for large values of the rotation normal coordinate, the rotating atoms will disappear into infinity, and this is not what we call a rotation.

It is possible to define non-linear normal coordinates by expressing them in non-linear internal coordinates, *e.g.* a pure bending. This is what Jones and Coon did for the out-of-plane bending of formaldehyde (see eq. (3.2)); it is, however, not clear if with this non-linear coordinate eq. (2.31) will be satisfied better. If we use the non-linear coordinate for the out-of-plane bending, this implies that we have to use a different fourth column in the $(L^{-1}BM^{-1})'$ matrix (also used to transform the coupling components), at every point of the non-linear coordinate. The question will be taken up again with the discussion of the Results in Chapter 4.1.

We can describe the D_2CO molecule by assuming that the
normal modes are equal to those of H_2CO, except for a
constant depending on the mode considered. The following
relations hold:

$$\left. \begin{array}{l} V = \frac{1}{2} \omega^2 Q^2 \\ V = \frac{1}{2} (\omega^i)^2 (Q^i)^2 \end{array} \right\} \rightarrow Q^i = \frac{\omega}{\omega^i} Q \qquad (3.9)$$

The i-superscripted quantities are for D_2CO, the others
for H_2CO. For the program that calculates the vibration
functions, it is more convenient to use the same Q for
D_2CO, but to change the reduced mass from one to $\mu^i = \left(\frac{\omega}{\omega^i}\right)^2$
because this gives the same potential V, but the right
frequency:

$$V = \frac{1}{2} \mu^i (\omega^i)^2 Q^2 = \frac{1}{2} \omega^2 Q^2 \qquad (3.10)$$

The normal coordinates are different for D_2CO, therefore
the $(L^{-1}BM^{-1})'$ matrix will change as well:

$$x = (\mathcal{L}^{-1}\mathcal{B}M^{-1})' Q = (\mathcal{L}^{-1}\mathcal{B}M^{-1})' \frac{\omega^i}{\omega} Q^i = (\mathcal{L}^{-1}\mathcal{B}M^{-1})^i Q^i \qquad (3.11)$$

So $\quad (\mathcal{L}^{-1}\mathcal{B}M^{-1})^i = \frac{\omega^i}{\omega} (\mathcal{L}^{-1}\mathcal{B}M^{-1})' \qquad (3.12)$

The μ^i's for the six normal modes of D_2CO are listed in
Table 3.2; the ω's are taken from ref. 40.

mode	$\mu^i = (\frac{\omega}{\omega^i})^2$
1	1.8307
2	1.0548
3	1.8396
4	1.5484
5	1.7326
6	1.5913

Table 3.2.

3.2. Calculation of the Electronic Wavefunction and Proper-
ties

3.2.0. General

In this chapter we will show how equation (1.25) is
solved for formaldehyde:

$$(H_o - \mathcal{E}_i) \phi_i = 0 \qquad (3.13)$$

in which H_0 assumes the forms:

$$H_o = T_E + U(q, Q) \quad \text{and} \quad H_o = T_E + U(q, Q_o) \qquad (3.14)$$

for the ABO and CBO set, respectively.

Now:

$$T_E = \sum_{i=1}^{3N} \frac{\partial^2}{\partial q_i^2}$$

$$U(q, Q) = - \sum_{\ell=1}^{N} \sum_{m=1}^{k} \frac{z_m}{r_{\ell m}} + \sum_{\ell=1 < \ell'=1}^{N} \sum \frac{1}{r_{\ell\ell'}} + \sum_{m=1 < m'=1}^{k} \sum \frac{z_m \cdot z_{m'}}{R_{mn'}} \qquad (3.15)$$

in which q_i are the cartesian components of the electron
coordinates, N is the number of electrons, K is the number
of nuclei, Z_n is the charge of nucleus n.

r_{en} is the distance between electron e and nucleus n

r_{ee}' is the distance between electron e and electron e'

$R_{nn'}$ is the distance between nucleus n and nucleus n'

So we have to solve a partial differential equation of the
second order in 3N coordinates.

Fock[8] and Slater[9] simultaneously developed a method for
solving this equation; this method was based on earlier
work by Hartree[10] and is therefore known as the Hartree-
Fock method.

In the Hartree-Fock method we first put a constraint on the
function ϕ_i, in the sense that ϕ_i is written as a single
anti-symmetrized product of one-electron spin functions
(functions that depend only upon the spatial and spin coor-

dinates of one electron); antisymmetrical because electrons
are spin-half particles.

$$\phi_i = \mathscr{A} \prod_{i=1}^{N} S_i(\mu) \qquad (3.16)$$

A is the antisymmetrizer.
This is also called a Slater determinant of the functions
$S_i(\mu)$ or a configuration.
We write $S_i(\mu)$ as a product of a spatial orbital θ_i and a
spin function $\alpha(\mu)$ or $\beta(\mu)$ (the θ_i are also known as
molecular orbitals: MO's):

$$S_i(\mu) = \theta_i(\mu) \cdot \alpha(\mu) \quad or \quad \theta_i(\mu) \cdot \beta(\mu) \qquad (3.17)$$

We consider the special case of a closed shell system, $i.e.$:
an even number of electrons, each spatial orbital occurring
one time with α-spin and one time with β-spin.
Fock suggested a functional J that is stationary with res-
pect to the $\theta_i(\mu)$, for those θ_i that make ϕ_i a solution of
equation (3.13). This functional J can be given the physic-
al interpretation of the energy of the system if ϕ_i is the
solution of (3.13).

$$J = \frac{\langle \phi_i / H_o / \phi_i \rangle}{\langle \phi_i / \phi_i \rangle} \qquad (3.18)$$

Varying the functional J with respect to the θ_i, and putting
the variation in J equal to zero, gives the Hartree-Fock
equations:

$$\left[h(\mu) + \sum_{j=1}^{iN} (2 J_j - K_j) \right] \theta_i = \epsilon_i \theta_i \qquad (3.19)$$

or $\quad \mathscr{F} \cdot \theta = \epsilon \cdot \theta \quad$, ϵ is a diagonal matrix.
$h(\mu)$ is the one-electron part of the Hamiltonian for elec-
tron μ .

$$J_i(\mu) \cdot \theta_j(\mu) = \langle \theta_i(\nu) \mid \frac{1}{r_{\mu\nu}} \mid \theta_i(\nu) \rangle_\nu \cdot \theta_j(\mu)$$

$$K_i(\mu) \cdot \theta_j(\mu) = \langle \theta_i(\nu) \mid \frac{1}{r_{\mu\nu}} \mid \theta_j(\nu) \rangle_\nu \cdot \theta_i(\mu)$$

(3.20)

The Hartree-Fock equations must be solved in an iterative
way. For atoms the equations can be integrated numerically,
for multi-center systems (more than one nucleus) this be-
comes impossible.
Roothaan[11] has solved the HF equations by expanding the
functions θ_i in a complete basis set of one-electron func-
tions:

$$\theta_i = \sum_p \eta_p \cdot c_{pi} = \eta^\dagger \, c_i$$

(3.21)

Substitution in the functional J and varying now with res-
pect to the C's gives the HF equations in linear form, in-
stead of differential form:

$$\mathcal{F} \, c_i = \epsilon_i \, \Delta \cdot c_i$$

(3.22)

in which
$$\mathcal{F} = \eta^\dagger \mathcal{F} \eta$$

$$\Delta = \eta^\dagger \eta$$

and
$$F_{pq} = \langle \eta_p(\mu) \mid h(\mu) \mid \eta_q(\mu) \rangle + \sum_{j=1}^{\frac{1}{2}N} \left[2\langle \eta_p(\mu) \mid J_j(\mu) \mid \eta_q(\mu) \rangle + \right.$$
$$\left. - \langle \eta_p(\mu) \mid K_j(\mu) \mid \eta_q(\mu) \rangle \right]$$
$$= h_{pq}(\mu) + \sum_{h,s} R_{h,s} \left[2\langle \eta_p(\mu) \, \eta_s(\nu) \mid \frac{1}{r_{\mu\nu}} \mid \eta_q(\mu) \, \eta_h(\nu) \rangle + \right. \quad (3.23)$$
$$\left. - \langle \eta_p(\mu) \, \eta_s(\nu) \mid \frac{1}{r_{\mu\nu}} \mid \eta_h(\mu) \, \eta_s(\nu) \rangle \right]$$

with
$$R_{h,s} = \sum_{j=1}^{\frac{1}{2}N} c_{hj} \cdot c_{sj} \quad, \text{ the first order density matrix.}$$

This is a pseudo eigenvalue equation in which the c_i form
the pseudo eigenvectors. This equation can be solved with
a variety of numerical procedures[12].

For the basis functions η one used initially so-called
Slater functions:

$$\eta_{m\ell} = R^{m-1} \cdot e^{-\frac{\xi}{n} \cdot R} \cdot Y_\ell^m(\theta,\varphi) \qquad (3.24)$$

$Y_1^m(\theta, \phi)$ is a spherical harmonic in real form.
ξ is a number that is given the physical interpretation of
an effective nuclear charge.
These Slater functions were used because they express in
analytical form the numerical solutions of the Hartree
equations (the Hartree equations are similar to the HF
equations with the difference that the ϕ_i are not anti-
symmetrized).
A disadvantage of the Slater functions is that multi-center
integrals are very time-consuming to evaluate. Therefore,
we use a basis set of cartesian Gaussian functions:

$$\eta_{m_1, m_2, m_3} = e^{-\alpha R^2} \cdot x^{m_1} \cdot y^{m_2} \cdot z^{m_3} \qquad (3.25)$$

These functions can be integrated a lot easier, but more
functions are necessary to obtain the same accuracy as with
the Slater functions. This has an especially time-consuming
effect on the iterative solution of the HF equations, be-
cause of the increased size of the HF matrix. Therefore,
the basis functions are grouped, and we obtain the so-
called contracted basis functions:

$$\eta_i' = \sum_j \eta_j \cdot d_{ji} \quad , \quad i = 1, \ldots, \text{number of contracted} \qquad (3.26)$$
$$\text{functions.}$$

in which the d_{ji} are constant coefficients.
This reduces the size of the HF matrix and thus results in
a considerable saving of computing time.
One distinguishes single ζ, double ζ and extended basis
sets according to the number of basis functions used. As a
reference one takes the solutions of the hydrogen atom (1s,
2s, 2p etc.) and takes the number of these so-called atomic

orbitals (AO's), necessary to accomodate the electrons
available for a certain atom. A calculation done with this
number of STO's (Slater Type Orbitals) is of single ζ
quality. If two STO's per AO are taken one has double ζ
quality, more than two is called an extended basis set.
Going back to the solution of the HF equations, we realize
that the one-configuration constraint on ϕ_i can be re-
laxed. The reason is that the one-electron functions θ_i,
determined with the HF equations, form a complete set of
one-electron functions if the basis set η_p is complete.
Now ϕ_i is an N-electron function and we can prove that any
ϕ_i can be expressed as:

$$\phi_i(1, \dots, N) = \sum_{k_1 < k_2 < \dots < k_N} \left[\mathcal{A} \, \theta_{k_1}(1) \dots \theta_{k_N}(N) \right] \cdot C_{k_1, \dots, k_N}$$

(3.27)

$$= \sum_k D_k \cdot C_k$$

That is ϕ_i can be expressed as a sum of all possible con-
figurations that can be formed from the set θ_i.
In practice we work of course with only a finite number of
configurations in which hopefully only a few will pre-
dominate.
The coefficients C_k are determined by applying the varia-
tion method to the functional:

$$J = \frac{\langle \phi_i | H_o | \phi_i \rangle}{\langle \phi_i | \phi_i \rangle}$$

This gives the secular equations:

$$\sum_L (H_{kL} - \epsilon \, S_{kL}) = 0$$

in which $H_{kL} = \langle D_k | H_o | D_L \rangle$ (3.28)

and $S_{kL} = \langle D_k | D_L \rangle$

These secular equations again are a pseudo-eigenvalue pro-
blem that can be solved with known methods[12].

3.2.1. The AO Basis Set

The basis set used for the calculation of the electronic wave function of formaldehyde is a contracted Gaussian basis set. We used the exponents and contraction coefficients recommended by Dunning[4]. For carbon and oxygen we used a (9s5p) [4s3p] set, for hydrogen a (4s) [2s] set. (This set is of double ζ quality). The exponents and coefficients used are shown in Table 3.3.

carbon		oxygen		hydrogen	
exponents	coeffi-cients	exponents	coeffi-cients	exponents	coeffi-cients
4232.6100	0.002029	7816.5400	0.002031	13.3615	0.032828
634.8820	0.015535	1175.8200	0.015436	2.0133	0.231208
146.0970	0.075411	273.1880	0.073771	0.4538	0.817238
42.4974	0.257121	81.1696	0.247606	0.1233	1.0
14.1892	0.596555	27.1836	0.611832		
1.9666	0.242517	3.4136	0.241205		
5.1477	1.0	9.5322	1.0		
0.4962	1.0	0.9398	1.0		
0.1533	1.0	0.2846	1.0		

Table 3.3.

The integrals were calculated with the integral program of the IBMOLH program package[5].

3.2.2. The SCF Method

With the S(elf) C(onsistent) F(ield) method one determines in an iterative way the M(olecular) O(rbitals) that are the solution of the H(artree) F(ock) equations (eq. (3.22)) for a given state of the molecule, *i.e.* the ground

state or some excited state. These MO vectors are used to
perform the C(onfiguration) I(nteraction) calculation (eq.
(3.28)).

If the AO basis set is complete (*i.e.* the SCF solution
then is the HF limit) and the CI is also complete (*i.e.* all
possible configurations are used), then it does not make
any difference for which molecular state the MO vectors
are calculated. Both these conditions are not satisfied
for the present calculation of formaldehyde. Buenker and
Peyerimhoff[6] have investigated the effects of different
MO sets in the CI calculation of formaldehyde. Their con-
clusion is that a given state is described best if the MO-
vectors used in the CI calculation, are obtained from an
SCF on the same state (so-called parent state MO's: PSMO's).
If one uses GSMO's (ground state MO's) to describe the $^1A_2$
and $^3A_2$ excited states in a CI calculation, then the non-
planar equilibrium geometry is not found and the excitation
energy for these states overestimated (4.71 eV *versus* 3.44
eV).

For the present purpose it is necessary to use one MO set
to calculate both the ground and excited state. The reason
is that transition properties are calculated between the
two states (see 3.2.5); if two different MO sets are used,
then rather time-consuming manipulations must be performed
to calculate the transition properties[7].

In order to describe ground and excited state with the same
accuracy with one MO set, we have to obtain an MO set
that is in some way intermediate between those of ground
and excited state. One way of doing this is to use the
Transition Orbital Method (TOM) developed by Goscinski *et*
al.[13-19]. This method is especially suited for single exci-
tations, *i.e.* excitations in which one electron is promoted
from MO i to MO a. The HF operator is then changed in such
a way that effectively one half electron is removed from
the MO i, and one half electron is put into MO a. We work
with the RHF method in which we then have 1.5 electrons in
i and 0.5 electron in a. Also because of the RHF method we

have 0.75 α electron and 0.75 β electron in i, and 0.25 α
and 0.25 β electron in a.
In the normal RHF procedure the HF operator has the form[39]
(see eq. (3.19)):

$$\mathscr{F} = h(\mu) + \sum_{j=1}^{iN} (2 J_j - k_j) \tag{3.29}$$

in the η basis this gives[39]: (cf. eq. (3.23))

$$F_{pq} = h_{pq}(\mu) + \sum_{\lambda, s} R_{\lambda, s} \left[2 \langle ps \| q\lambda \rangle - \langle ps \| \lambda q \rangle \right] \tag{3.30}$$

with
$$R_{\lambda, s} = \sum_{j=1}^{iN} c_{\lambda j} \cdot c_{sj}$$

The HFTOM operator has the form:

$$\mathscr{F}^T = h(\mu) + \sum_{\substack{j=1 \\ \neq i}}^{iN} (2 J_j - k_j) + \tfrac{3}{4}(2J_i - k_i) + \tfrac{1}{4}(2 J_a - k_a) \tag{3.31}$$

This results in:

$$F_{pq}^T = h_{pq}(\mu) + \sum_{\lambda, s} R_{\lambda, s}^T \left[2 \langle ps \| q\lambda \rangle - \langle ps \| \lambda q \rangle \right] \tag{3.32}$$

with
$$R_{\lambda s}^T = \sum_{j=1}^{iN, a} c_{\lambda j} \cdot c_{sj} - \tfrac{1}{4} c_{\lambda i} \cdot c_{si} - \tfrac{3}{4} c_{\lambda a} \cdot c_{sa}$$

The Transition Operator Method was developed by Goscinski
et al. to be able to calculate transitions energies with
one calculation instead of the usual two. But they indeed
suggest that the TOM orbitals should form a suitable basis
for performing CI calculations in which two states are to
be described correctly[14],[19].
The SCFV program[5] was changed, so that TOM functions can
be calculated.

3.2.3. The CI Method

Only a limited number of configurations can be admitted in the CI calculation. The problem is how to select these configurations. We use the "point" system of Morokuma and Konishi[20,21]: "In this system, each MO is assigned a point based on its energy and its supposed importance for the properties being calculated. Then each configuration is assessed a point that is the sum of the points of all MO's involved in the excitation from the reference (or ground) configuration". All configurations with points not greater than a chosen limit are included in the CI calculation.

For formaldehyde we take the points for the MO's from reference 21. The points are: 3,3,2,1,1,1,1,0,0,0,1,2 (in order of increasing energy of the MO's). The maximum sum of points allowed for any configuration is 2. We included 175 configuration in the CI calculation. The computer program consists of two parts: 1) a program to calculate the spin symmetry coefficients[5]; 2) a program to generate the H-matrix and diagonalizing it[5].

3.2.4. The Crude Adiabatic Wave Function

The CBO function is defined by eq. (1.23). From eq. (2.22) we have that:

$$U(q,Q) - U(q,Q_0) = V_{en}(q,Q) - V_{en}(q,Q_0)$$

So for each Q we only have to evaluate:

$$\left\langle \phi_m(q,Q_0) \,\middle|\, V_{en}(q,Q) \,\middle|\, \phi_n(q,Q_0) \right\rangle_q \tag{3.33}$$

This expression consists only of one-electron integrals; there is an enormous time-saving compared with the ABO function, also because we only have to calculate the wave

function in the equilibrium position Q_0. We modified the
IBMOL program[5] so that these integrals were evaluated,
while we took for the $\phi_n(q,Q_0)$ the ABO CI function of the
equilibrium position Q_0.

3.2.5. The Properties

A. The ABO set

We have adapted the properties program of the POLY-
ATOM package[5], so that properties between CI functions can
be calculated.
For each point of the energy surface   where the wave
function of ground and excited state are calculated, we
calculate the 12 cartesian components (3 per atom) of the
electric field operator, and the 3 components of the dipole
operator. So we have:

$$\langle \phi_0 \,/\, \mathscr{P} \,/\, \phi_1 \rangle_Q \tag{3.34}$$

in which P is an operator and ϕ_0 and ϕ_1 are CI functions.
The 12 cartesian components of the electric field operator
are transformed to 12 normal coordinate components (see
Table 3.1). The electronic dipole transition element can
be expressed in three ways[22,35]:

dipole length: $\quad {}^L\!\mathscr{D}(Q) = \langle \phi_1 \,/\, \sum_i q_i \,/\, \phi_0 \rangle_Q \tag{3.35}$

dipole velocity: ${}^V\!\mathscr{D}(Q) = \{ \mathscr{E}_0(Q) - \mathscr{E}_1(Q) \}^{-1} \langle \phi_1 \,/\, \sum_i \nabla_i \,/\, \phi_0 \rangle_Q \, , \, \nabla_i = \frac{\partial}{\partial q_i} \tag{3.36}$

dipole acceleration: ${}^A\!\mathscr{D}(Q) = \{ \mathscr{E}_0(Q) - \mathscr{E}_1(Q) \}^{-2} \langle \phi_1 \,/\, \sum_i (\nabla_i V) \,/\, \phi_0 \rangle_Q \tag{3.37}$

For the symbols used see 2.2.1 (q_i and ∇_i are defined with
respect to the origin of the coordinate system as are the
other terms of the Hamiltonian).

The transition dipole moments are invariant to the choice of the origin. The dipole transition moment is given by:

$$D = \langle \chi_{1p}(Q) \mid D(Q) \mid \chi_{0q}(Q) \rangle_Q \tag{3.38}$$

If D(Q) can be written as:

$$D = D(Q_o) + \sum_k D(Q_k) \tag{3.39}$$

then

$$D = D(Q_o) \cdot \prod_m \langle \chi_{1p}(Q_m) \mid \chi_{0q}(Q_m) \rangle + $$
$$+ \sum_k \prod_{m \neq k} \langle \chi_{1p}(Q_k) \mid D(Q_k) \mid \chi_{0q}(Q_k) \rangle \cdot \langle \chi_{1p}(Q_m) \mid \chi_{0q}(Q_m) \rangle \tag{3.40}$$

The oscillator strength can be expressed in D:

$$f = \frac{2m_e}{3\hbar^2 e^2} \cdot \Delta E \ |D|^2 \quad , \quad m_e = \text{electron mass} \tag{3.41}$$
$$e = \text{"} \quad \text{charge}$$

in atomic units we get:

$$f = \frac{2}{3} \ \Delta E \cdot |D|^2 \tag{3.42}$$

in which ΔE is the energy difference between initial and final state. The radiative lifetime for spontaneous emission is:

$$\tau_r = \frac{1}{A_{kl}} \quad , \quad \text{with} \quad A_{kl} = \frac{2\Delta E^3}{\pi c^3 \hbar^2} \cdot B_{kl} \tag{3.43}$$

(A_{kl} and B_{kl} are Einstein coefficients)
Now:

$$B_{kl} = \frac{2\pi e^2}{3\hbar^2} \cdot |D|^2 \rightarrow A_{kl} = \frac{4\Delta E^3}{3c^3\hbar^4} \ |D_{kl}|^2$$

So:

$$\tau_h = \frac{3c^3\hbar^4}{4\Delta E^3 |D_{hl}|^2 l^2} \tag{3.44}$$

τ_r is an experimental quantity that is known for several levels of formaldehyde.
L_D and A_D are calculated.
A_D can be simply expressed in $E_j^{1;0}_n$ (see eq. (2.15)):

$$^{A}D^{j'}(Q) = -\{\Phi_0(Q) - \Phi_1(Q)\}^{-2} \sum_m E_{j'n}^{1,0} \cdot Z_m \tag{3.45}$$

Z_n is the charge of nucleus n.
$A_D j'$ is the j'th component of A_D.

B. The CBO Set

From eq. (2.26) we know that there is only one compo-
nent of the coupling element; it is also calculated with
the CI properties program using for $\phi_n(q,Q_0)$ the ABO CI
function in the equilibrium point Q_0.
The transition dipole moment is of course zero in the case
of formaldehyde (forbidden transition), because no account
is taken of the coupling of the CBO function with higher
electronic states.

3.3. Calculation of the Vibrational Wave Function and Properties

3.3.0. General

We have to solve the vibrational wave equation for
each normal coordinate Q_k:

$$\{T_N + \Phi_i(Q_k) - E_{im}^k\} \chi_{im}(Q_k) = 0 \tag{3.46}$$

(see also eq. (2.30) and following)

in which $T_N = \frac{1}{2} \frac{\partial^2}{\partial Q_k^2}$; Q_k being a mass-weighted normal coordinate.

With the COUPEL program (see 3.3.1) we first solve this equation for the lowest vibrational states of the excited electronic state, *i.e.* i = 1, n = 0,1,2,...; k = 1,...,6. We then select the vibrational wave function of interest, say n = 1, and calculate the energy of it:

$$E_{1,1} = \Phi_1(Q_0) + \sum_k E_{1,1}^k \qquad (3.47)$$

We now solve the vibrational equation for the 6 normal coordinates of the ground state, for eigenvalues until   . So i = 0, k = 1,...,6 and $E_{on}^k \lessgtr E_{1,1}$.

We feed the eigenvalues $E_{o,n}^k$ (k = 1,...,6, n = 0,1,...) in the VICTBAR program (see 3.3.2).

We also indicate an energy interval ΔE around $E_{1,1}$. The program finds all combinations of the six vibration functions (one for each normal coordinate), that have a total energy in the specified interval ΔE (this we call the "raw" density of energy levels). ΔE is chosen so that an increase in ΔE does not influence the decay function P(t); ΔE will have to be of the order of $\frac{\pi v^2}{\epsilon}$ (see 2.3) if the Bixon-Jortner model is valid.

For each of these total vibration functions we calculate the coupling with the total vibration function of the excited state with the COUPEL program (see 3.3.3). In order to do this, the program needs, apart from the vibration functions of ground and excited state, also the coupling elements for each point of the six potentials. For ABO functions the coupling element has six components per point, for CBO functions only one component.

Having obtained all vibration functions in the energy interval ΔE, each with its energy and coupling element, these data are fed into the INTERF program (see 3.4). This

program calculates the exact eigenfunctions by diagonaliz-
ing the interaction matrix. It also calculates the time-
dependence of the oscillator strength, if all these eigen-
functions are excited on t = 0. This decay function can be
compared with the experimental decay curve.

3.3.1. The Vibrational Wave Function

In the COUPEL (Coupling Element) program the vibra-
tional eigenfunctions and eigenvalues are calculated by
numerical integration of the vibrational wave equation.
The integration procedure is taken from the TRAPRB program
written by W.R. Jarmain and J.C. McCallum[23,24,25]. Jarmain
and McCallum slightly modified the program of Zare and
Cashion[26], who modified the program written by Cooley[27].
The method they used was given by Hartree[28], who based it
on the Numerov finite difference method[42]. An idea about
the accuracy of the obtained wave function can be acquired
from the orthogonality test.

$|\langle \chi_1 | \chi_2 \rangle|$ is of the order of 10^{-12}

The number of integration points is 200-800 per Å, depend-
ing on the number of nodes the wave function contains. The
potential energy curve is calculated in all these points
by fitting cubic splines to the points calculated with the
ab initio CI program.

3.3.2. The Energy Levels of the Total Vibrational Wave
       Function

We need to know the energies $E_{0,n}$:

$$E_{on} = \Phi_o(Q_o) + \sum_k E_{o,n}^k \qquad (3.48)$$

that lie in a certain predetermined energy interval ΔE. To

this end the algorithm VICTBAR[*] (Vibrational Counting with Backtracking Algorithm) was developed[29], which is based on the backtracking procedure from combinatorics[30]. This method has many advantages over the methods used in the literature[29]. The program can accommodate both the harmonic and the anharmonic case, with and without degenerations. All that is required are the positions of the energy levels in each of the normal modes. It turns out that deviations from the harmonic potential have a large effect on the level density (see 4.2), contrary to what has been maintained in the literature[31,32].

3.3.3. The Vibrational Integrals

The vibrational coupling for the ABO set (see eq. (2.36)) and the CBO set (eq. (2.42)) are implemented in the COUPEL program. The integrals that occur in these expressions are of the following types:

$$\langle \chi_{ip}(Q_k) | \chi_{of}(Q_k) \rangle$$
$$\langle \chi_{ip}(Q_k) | V(Q_k) | \chi_{of}(Q_k) \rangle$$
$$\langle \chi_{ip}(Q_k) | \frac{\partial}{\partial Q_k} | \chi_{of}(Q_k) \rangle \tag{3.49}$$
$$\langle \chi_{ip}(Q_k) | V(Q_k) \frac{\partial}{\partial Q_k} | \chi_{of}(Q_k) \rangle$$

All these integrals are evaluated numerically with an integration grid of 200-800 points per Å (depending on the number of modes the wave functions contain). The coupling elements are calculated at all these points by fitting cubic splines to the points known from the *ab initio* CI calculation.

---

[*] Not to be confused with Victor Baarn, a mysterious cash collector[43].

The integration is performed with the modified trapezium
rule:

$$\int_a^b f(x)\, dx = \left\{ \sum_{i=0}^{N} f_i \right\} \cdot \Delta x \qquad (3.50)$$

with $\quad f_i = f(x_i) = f(a + i * \Delta x) \ ; \ \Delta x = \dfrac{b-a}{N}$

The differentiation is performed with a four point rule[33]:

$$Df(h) = \left\{ -f(2h) + 8f(h) - 8f(-h) + f(-2h) \right\} / 12\, h \qquad (3.51)$$

Some tests were performed to determine the dependence of
the overlap integrals on the exact form of the potential.
Overlap integrals were calculated between the vibration
functions of two different potentials. One vibration func-
tion had a low energy (zero nodes), the other was highly
excited (30 nodes); this situation resembles the formalde-
hyde case. The potential energy curve for the 30 node
function was varied and the effect upon the overlap inte-
gral evaluated. It was found that the overlap integral is
determined primarily by the lower part of the potentials.
Variations in the higher part of the potential energy
curve gave variations in the overlap integral of 150%,
while corresponding variations in the lower part resulted
in deviations of 600%. This is due to the fact that the
zero-node wave function differs from zero only around the
equilibrium configuration; so when determining the overlap
integral, only this part of the 30-node wave function is
important; now the 30-node wave function around the equi-
librium configuration is primarily determined by the poten-
tial energy curve in this region.
From all this it follows that, despite the fact that we
are working with highly excited vibration functions, the
lower part of the potential curve is the most important
part for the properties we are interested in.
If we want to describe the lowest part of the potential
energy curve, then the normal coordinates provide the best

choice.

If we want to describe the higher part of the potential energy curve, then internal coordinates[*] are better.

3.4. Calculation of the Radiationless Decay

A set of equations of the following form has to be solved to obtain the non-BO states (see eq. (2.43)):

$$
\begin{pmatrix}
E-E_0 & \nu_1 & \nu_2 & , & \cdots & , & \nu_N \\
\nu_1 & E-E_1, & & & & & \\
\nu_2 & & E-E_2, & & \bigcirc & & \\
\vdots & & & \ddots & & & \\
\nu_N & & \bigcirc & & & & E-E_N
\end{pmatrix}
\begin{pmatrix}
a_0 \\
a_1 \\
a_2 \\
\vdots \\
a_N
\end{pmatrix}
=
\begin{pmatrix}
0 \\
0 \\
0 \\
\vdots \\
0
\end{pmatrix}
\tag{3.52}
$$

The secular equation is:

$$
f(E) = (E-E_0) + \sum_{i=1}^{N} \frac{\nu_i^2}{E_i - E} = 0
\tag{3.53}
$$

Normalization of the eigenfunctions requires:

$$
a_0^2 + \sum_{i=1}^{N} a_i^2 = 1
\tag{3.54}
$$

From (3.52) we also obtain:

$$
a_i = \frac{-\nu_i}{E-E_i} \cdot a_0 \quad , \quad i \geqslant 1
\tag{3.55}
$$

---

[*] Internal coordinates are also used under the name "local modes" for the analysis of the vibrationally highly excited part of the spectrum[36,37,38].

Combining (3.54) and (3.55) we obtain:

$$a_o^2 + \sum_{i=1}^{N} \frac{\nu_i^2}{(E-E_i)^2} \cdot a_o^2 = 1 \rightarrow a_o^{-2} = 1 + \sum_{i=1}^{N} \frac{\nu_i^2}{(E-E_i)^2} = f'(E) \rightarrow$$

$$a_o^2 = \frac{1}{f'(E)}$$

(3.56)

This is particularly fortunate, as we are only interested in a_0 (see 2.2).

The function f(E) has only one zero-point between each pair (E_i, E_{i+1}); f'(E)>1, we therefore find the zero-points with a Newton iteration procedure:

$$x_{n+1} = x_n - \frac{f(x_n)}{f'(x_n)}$$

(3.57)

in which X_{n+1} is the (n+1)th approximation for the zero-point.

The interference of the non-BO states is described by (see (2.46)):

$$P_1(t) = \langle \Psi_1(o) | \Psi_1(t) \rangle = \left| \sum_{k} (a_k)_o^2 \cdot \ell^{-iE_k t} \right|^2$$

(3.58)

The k in $(a_k)_0$ denotes the kth eigenvector.
$P_1(0)$ has to equal 1.

4. RESULTS AND COMPARISON WITH EXPERIMENT

4.1. The Vibrational Structure of the $^1A_1 \rightarrow {}^1A_2$ Radiative Transition

The energies of the ground and $(n\pi^*)$ excited state of formaldehyde were calculated as a function of the six normal coordinates. About 14 points per normal coordinate were calculated. Also were calculated for each point the 3 Cartesian components of the dipole transition moments $^L D$ and $^A D$. See Figure 4.1. for the potential energy curves. The point 0 in the figures is the point Q_0 of equation (2.31); for the point Q_0 was taken the experimental equilibrium point for the normal coordinate calculation of the ground state, which is shown in Figure 3.1.
The calculated equilibrium values for the $^1A_1$ and $^1A_2$ state for each of the internal coordinates are obtained from Fig. 4.1. They are compared with the experimental ones[1] in Table 4.1. (θ is the out-of-plane angle).

H_2CO

	$^1A_1$		$^1A_2$	
	experimental	calculated	experimental	calculated
θ deg.	0.0	0.0	33.6	30
HCH deg.	116.52	116.5	118.0	112.5
C-H A	1.1161	1.10	1.0947	1.06
C-O A	1.2078	1.23	1.3252	1.36

Table 4.1. The calculated equilibrium geometries

The dipole length moment in Q_0 for ground and excited state is shown in Table 4.2. To be completely comparable with ex-
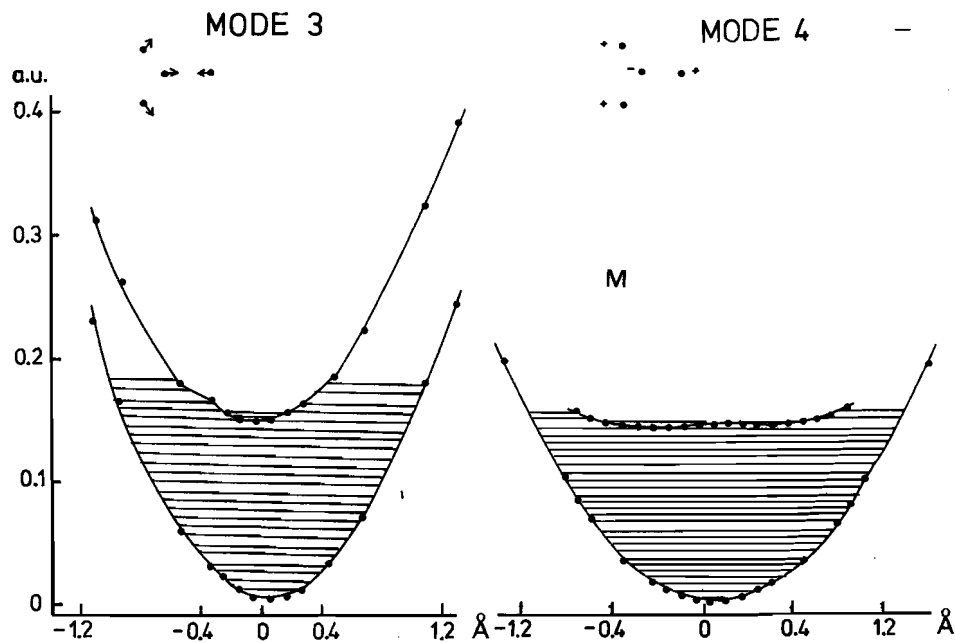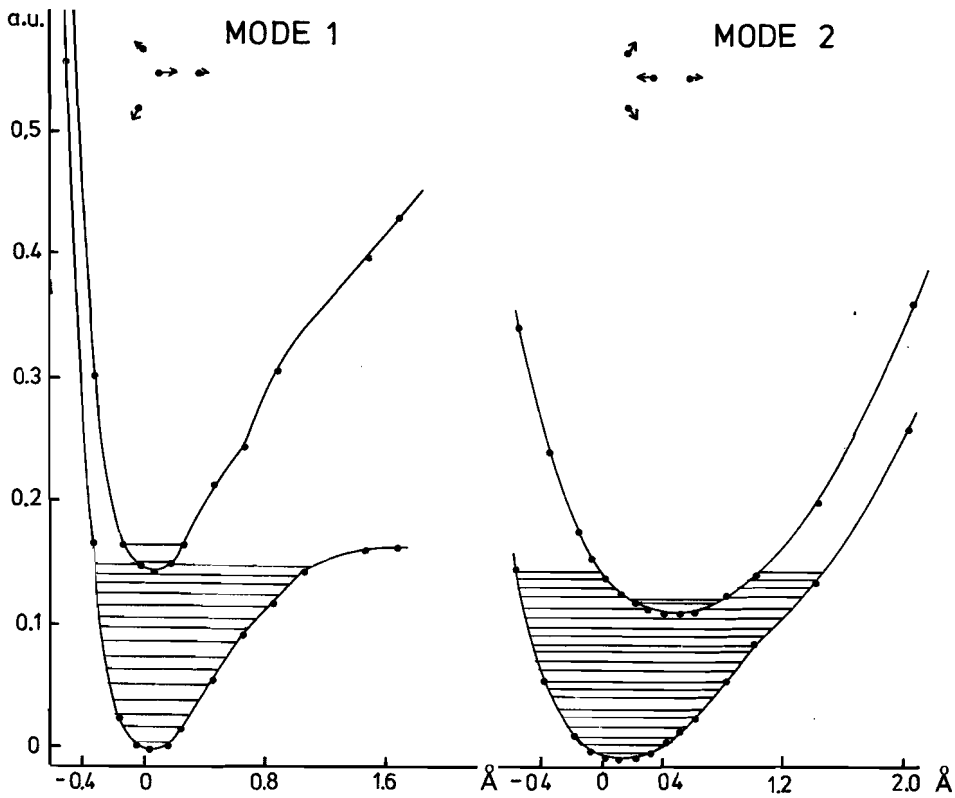
Fig. 4.1. a)
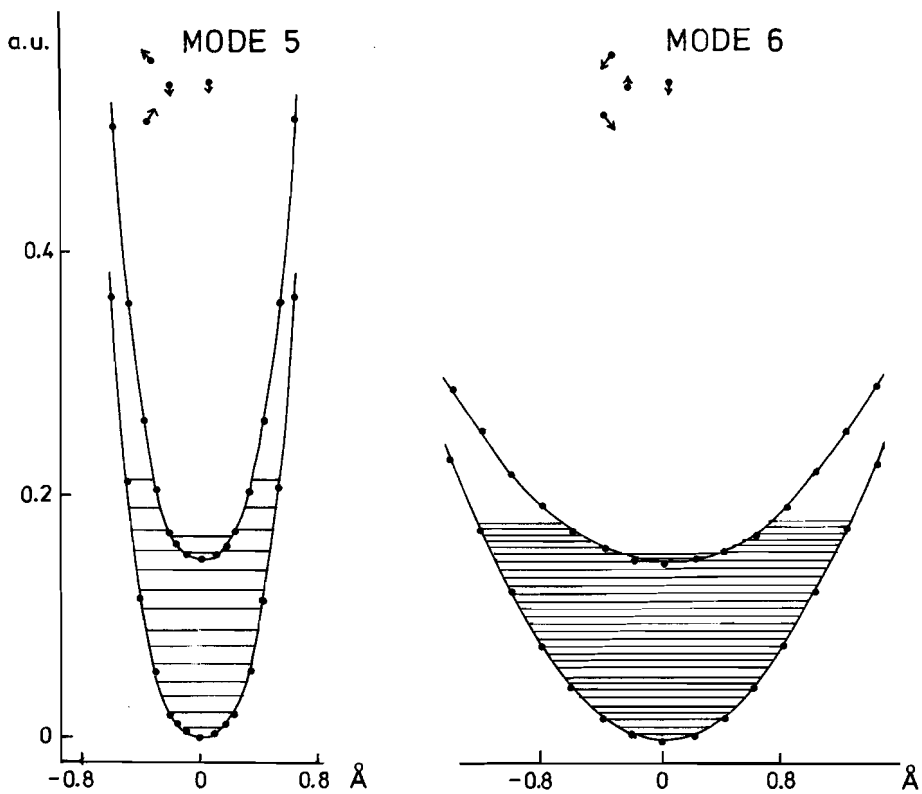
Fig. 4.1. b)

experiment, one has to calculate the dipole moment for the
zero vibrational state, which will lower the calculated
value somewhat.

dipole moment		
	calculated[a]	experimental
$^1A_1$	-1.114	-0.920[b]
$^1A_2$	-0.652	-0.614[c]

[a] calculated in Q_0
[b] from reference 3
[c] from reference 14

Table 4.2. The dipole moments

Concerning the calculation of the potential energy curves
for mode 4 the following can be remarked. We first used
the <u>linear</u> normal coordinate for the out-of-plane movement.
For the $^1A_2$ state this resulted in an energy lowering of
25 cm^{-1} (with as reference energy the energy in the point
Q_0) for an out-of-plane angle of 30°. Next we used the non-
linear out-of-plane coordinate (that leaves the bond
lengths intact, see Chapter 3.1.); using this coordinate
resulted in an energy depression of 157 cm^{-1}, again at 30°.
The experimental energy dip (from the frequencies of the
vibrational progression in mode 4 of the excited state) is
356 cm^{-1}. The difference is obviously caused by the fact
that in the calculations the equilibrium point Q_0 of the
excited state was taken the same as that of the ground
state: Q_0. This is of course an approximation (see Table
4.1.) and adversely affects all the excited state frequen-
cies (see Table 4.3.) but in particular mode 4, because of
the extremely small energy difference involved. We there-
fore used for the excited state potential of mode 4, the
experimentally determined energy curve[15,16]; the ground
state energy curve and the transition dipole and non-adia-
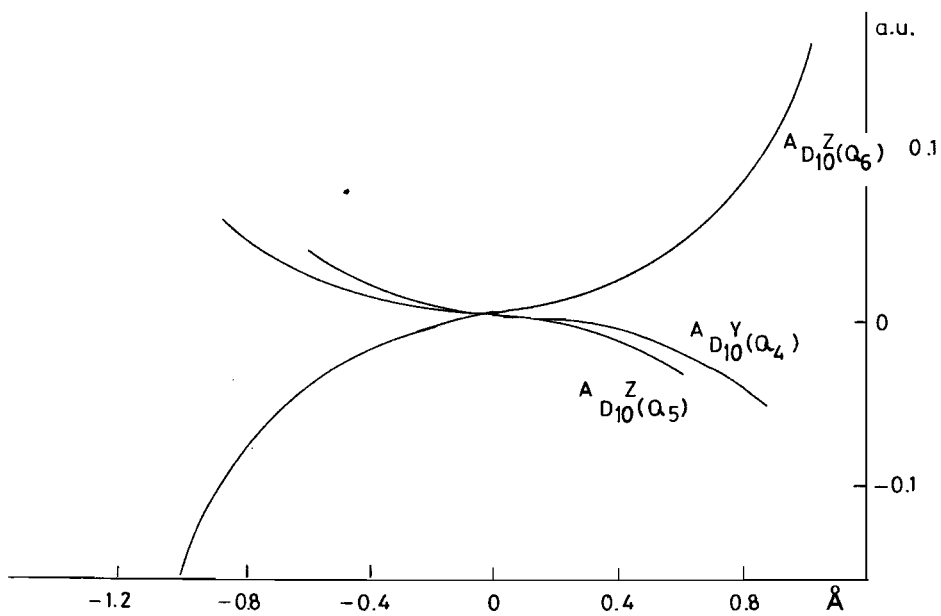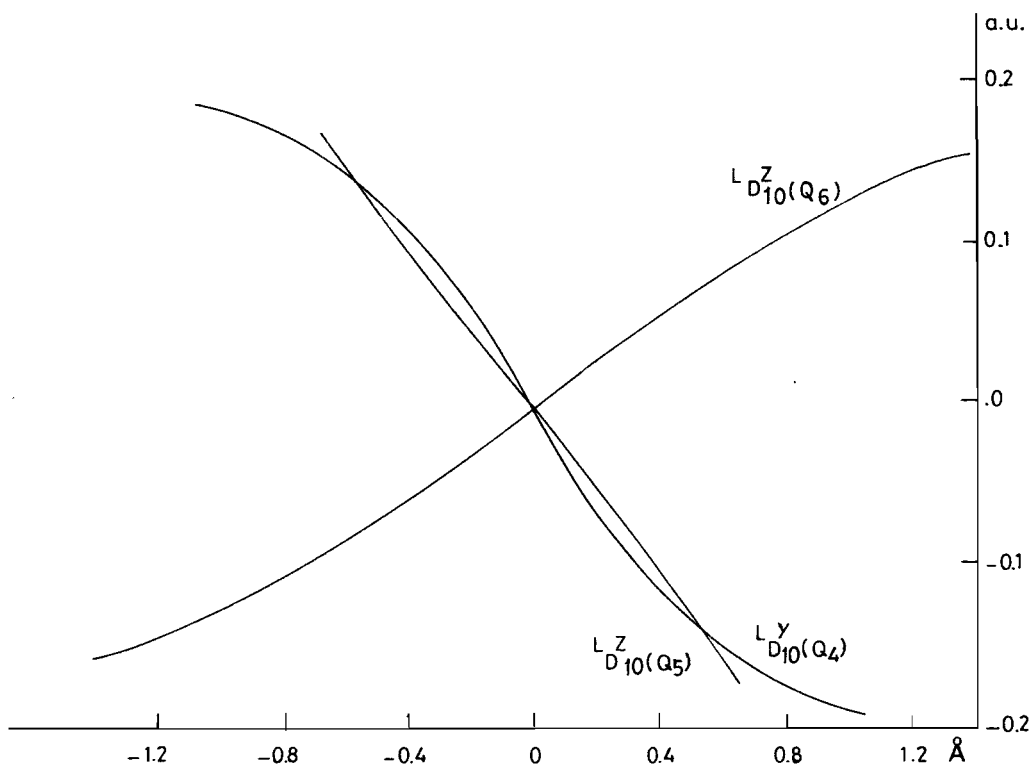
Fig. 4.2.

batic coupling elements were calculated with the electronic
wave functions obtained for the linear normal coordinate
path.

The zero-vibrational level energies for ground and excited
state of H_2CO and D_2CO are listed in Table 4.3.

Table 4.3. The zero-vibrational energy levels with as re-
ference energy the $\Phi_0(Q_0)$ and $\Phi_1(Q_0)$ energy for
the $^1A_1$ and $^1A_2$ state, respectively

mode	H_2CO		D_2CO	
	$^1A_1$	$^1A_2$	$^1A_1$	$^1A_2$
1	1345.4	1359.9	942.0	940.8
2	795.2	-5328.8	434.9	-5341.0
3	705.3	430.9	499.2	234
4	698.2	- 116.4[a]	575.8	- 144.6[a]
5	1302.9	1335.8	999.3	1018.0
6	661.1	490.8	523.8	388.5
Σ	5508.1	-1824.8	3975.0	-2904.3

[a] experimental values, see Discussion p. 63

The calculated 0-0 transition energy for H_2CO (see eq.
(2.33)):

$$\bar{\phi}_1(Q_o) - \bar{\phi}_o(Q_o) + \Sigma \nu_i \, {}'A_2 - \Sigma \nu_i \, {}'A_1 =$$

$= 32090.3 - 0 + (-1824.8) - 5508.1$
$= 32090.3 - 7332.9$
$= 24757.4 \text{ cm}^{-1}$

The experimental 0-0 transition lies at 28188 for H_2CO[15],
which is 3.49 eV = 0.1287 a.u. So there is an underestima-
tion of 3430.6 cm^{-1} = 0.0157 a.u., which is of the order of
magnitude for the error in a calculation of this type[10,11].
The calculated difference between the H_2CO and D_2CO 0-0
transition is -453.6; experimentally it is -113 cm^{-1}[15].

The calculated vibrational frequencies for the lowest IR
transitions in ground and excited state for H_2CO and D_2CO
are listed in Table 4.4., where they are compared with the
experimental data.

It appears that, apart from mode 3 in the excited state,
the calculation can reproduce the experimental results to
within 30-300 cm^{-1}; the largest discrepancy occurs for the
excited state mode 1.

Mode 3 of the excited state is particularly intriguing.
Experimentally the assignment of v_3 is rather problematic[15];
it is in fact based on only two bands: one type B band in
HDCO at 874 cm^{-1} from the 0-0 band, the other a type B hot
band in H_2CO at 262 cm^{-1} from the 0-0 band. The latter band
is by Job et $al.$ assigned to: 3_0^1 4_1^2, resulting in a v_3 =
887 cm^{-1}. We calculate, however, that the 3_0^1 4_1^0 band has an
intensity 17 times larger than the 3_0^1 4_1^2 band (see Table
4.7.); assigning 3_0^1 4_1^0 to this band results in a v_3 = 1429
cm^{-1}, which is in the expected range from the calculated
value of 1495.9 cm^{-1}.

The 874 cm^{-1} band in HDCO is assigned by Job et $al.$ to
3_0^1 4_0^1; however, this band does not occur in the H_2CO and
D_2CO spectrum at the required places.

Applying Teller-Redlich product rule ratios one obtains
for v_3 in D_2CO 1009 cm^{-1} and 1290 cm^{-1} in HDCO.
Sethuraman et $al.$[19] have deduced from the rotational fine
structure that the band in H_2CO, 262 cm^{-1} from the 0-0
band, has a type C Coriolis interaction with the $4^2 6^1$
band that lies 17 cm^{-1} above it. This finding is also com-
patible with the $3^1 4^0$ assignment of the 262 cm^{-1} band.

Formaldehyde is an asymmetric top molecule. Therefore,
there are three types of bands in the $^1A_1$ → $^1A_2$ absorption
spectrum: type A, B and C bands. These bands can be re-
cognized by the characteristic shape of the rotational fine
structure; the bands result from a transition moment along
the a, b and c axis, respectively. The a axis is defined
as the axis with the smallest moment of inertia (the x axis
in formaldehyde, see Fig. 3.1., p. **35**); the c axis as the

Table 4.4.

	H$_2$CO		D$_2$CO	
mode	exp.[a]	calcul.	exp.[a]	calcul.
$^1A_1$ state				
1_0^1 [d]	2766.4	2796.2	2055.8	2041.6
2_0^1	1746.1	1651.0	1700	1612.3
3_0^1	1500.6	1546.3	1105.7	1117.2
4_0^1	1167.3	1242.3	933.8	1004.1
5_0^1	2843.4	2656.0	2159.7	1974.8
6_0^1	1251.2	1325.5	990.4	1049.8
$^1A_2$ state				
1_0^1 [d]	2847	3157.7	2079	2348.9
2_0^1	1173	1345.0	1176	1309.8
3_0^1	887 (1429)[b]	1495.9	(625)[e] (1009)[b]	1107.2
4_0^1	124.6	125.9[c]	68.5	67.8[c]
4_1^2	417.7	419.4[c]	318.5	327.4[c]
4_2^3	405.6	408.5[c]	281.0	286.5[c]
5_0^1	2968	2767.2	2233	2070.4
6_0^1	904	988	705	781.3

[a] Experimental data from reference 15.

[b] Revised assignment, see Discussion p.**66**

[c] Calculated from the experimental potential, see Discussion p.**63**

[d] In this Table X$_0^1$ means a transition concerning only one electronic state.

[e] Not observed, but calculated from Teller-Redlich product rule ratios by Job *et al.*

one with the largest moment of inertia (the z axis in for-
maldehyde). The b axis has the intermediate moment of iner-
tia (the y axis in formaldehyde). The B and C bands of a
nearly symmetric top molecule become the perpendicular
bands of the symmetric top molecule; the A band becomes
the parallel band.

In formaldehyde the type A bands have an intensity of 3-5%
of the type B bands[15]. It is estimated from experiment that
the type B bands contribute 75% of the total oscillator
strength, the rest being type C.

From symmetry considerations[9] one can derive that mode 4
should give a transition moment along the y axis (type B
bands), and mode 5 and 6 along the z axis (type C bands),
all other transition moments being zero. This is also what
we find with our calculations; the resulting three transi-
tion dipole length and acceleration moments are shown in
Figure 4.2. It is observed in Figure 4.2. that the accele-
ration dipole transition moments are 3-80 times larger
than the corresponding length moments. This is a fact
well-known in the very few calculations that have so far
been done with the acceleration formula[20-23]. It turns out
that the acceleration formula depends very sensitively
upon the wave function close to the nuclei, because of the
$1/r^2$ term in the operator[24]. The dipole length form of the
transition moment depends more strongly on the wave func-
tion farther from the nuclei; therefore, the dipole length
form is always more accurate than the acceleration
form[20-23], because the wave functions usually calculated
are not designed to be accurate close to the nuclei. So
comparing the acceleration and length transition moments
gives an estimate of the accuracy of the electric field
transition components. From this comparison one estimates
that these electric field transition moments are probably
a factor 3 to 80 too large.

The electric field components for the ground state of for-
maldehyde have been calculated by Neumann and Moscowitz[25]
with a HF function using a basis set of double zeta plus

polarization functions. Our calculation gives results for these electric field components which differ at most 15% from their calculation.

In Tables 4.5. and 4.6. overlap integrals and transition dipole length integrals are listed. With formulas (3.40) and (3.41) we can calculate the oscillator strengths from it.

With Table 4.5. we can predict which "cold" (starting from χ_{00}) bands will occur in the UV spectrum of formaldehyde. First we have to remark that we are here only considering bands with type B or C polarization, as the type A bands are magnetic dipole transitions[15] or transitions caused by a combination of odd quanta in the B_1 (mode 4) and B_2 (mode 5 and 6) vibrations[15]. The latter combination transitions are not found with the present treatment, because it was assumed that the 6-dimensional integral for the transition moment can be approximated by a product of 6 one-dimensional integrals (see eq. (3.40)) ; to calculate the combination bands with A polarization, one would have to retain the two-dimensional integral over coordinates 4 and 5 or 4 and 6.

The following cold progressions (with polarizations) are predicted for H_2CO and D_2CO from Table 4.5:

$1^0_0 1^1_0$	(B or C polarization)		
$2^0_0 2^1_0 2^2_0 2^3_0 2^4_0 2^5_0 2^6_0$	("	"	)
$3^0_0 3^1_0$	("	"	)
$4^1_0 4^3_0 4^5_0$	(B	"	)
$4^0_0 4^2_0$	(C	"	)
5^0_0	(B	"	)
5^1_0	(C	"	)
6^0_0	(B	"	)
6^1_0	(C	"	)

Progressions are found in the spectra[15,29]; there are no experimentally found transitions with B or C polarization that are not found with the calculation. All calculated

Table 4.5.

mode	integral[a]	mole-cule	k=0	1	2	3	4	5	6
1	001k	H_2CO	0.98	0.17	0.37(- 1)	0.26(- 3)	-0.13(- 2)	0.16(- 2)	-0.31(- 3)
	001k	D_2CO	0.98	0.20	0.46(- 1)	0.25(- 2)	-0.18(- 2)	0.11(- 2)	0.59(- 3)
2	001k	H_2CO	0.31	-0.44	0.48	-0.45	0.37	-0.28	0.19
	001k	D_2CO	0.30	-0.44	0.48	-0.45	0.38	-0.28	0.20
3	001k	H_2CO	0.91	0.40	0.11	0.22(- 1)	-0.32(- 3)	-0.59(- 2)	-0.39(- 2)
	001k	D_2CO	0.88	0.45	0.16	0.43(- 1)	0.60(- 2)	-0.59(- 2)	-0.58(- 2)
4	001k	H_2CO	0.71	0.20(-4)	-0.64	0.64(- 5)	0.28	-0.82(- 5)	-0.11
	001k	D_2CO	0.62	0.71(-5)	-0.70	0.30(- 5)	0.33	-0.19(- 5)	-0.14
	00D1k	H_2CO	-0.20(- 5)	-0.23(-1)	-0.20(- 5)	-0.25(- 1)	0.18(- 6)	-0.15(- 1)	0.14(- 5)
	00D1k	D_2CO	-0.73(- 6)	-0.19(-1)	-0.69(- 6)	0.22(- 1)	-0.76(- 7)	-0.15(- 1)	0.38(- 6)
5	001k	H_2CO	1.0	0.49(-8)	0.93(- 2)	-0.19(- 8)	-0.52(- 3)	0.13(- 8)	-0.46(- 3)
	001k	D_2CO	1.0	0.47(-7)	0.10(- 1)	-0.51(-10)	0.68(- 4)	0.14(-10)	-0.56(- 3)
	00D1k	H_2CO	-0.12(- 9)	-0.21(-1)	-0.11(- 8)	-0.42(- 3)	0.20(-10)	-0.11(- 4)	-0.95(-11)
	00D1k	D_2CO	-0.13(- 9)	-0.19(-1)	-0.13(- 8)	-0.39(- 3)	0.14(-11)	-0.16(- 4)	-0.41(-12)
6	001k	H_2CO	0.99	0.36(-6)	-0.10	0.60(-10)	0.12(- 1)	0.35(- 8)	-0.15(- 2)
	001k	D_2CO	0.99	0.20(-6)	-0.82(- 8)	-0.19(- 7)	0.13(- 1)	0.55(- 8)	-0.16(- 2)
	00D1k	H_2CO	-0.59(-11)	0.16(-1)	0.73(-11)	0.28(- 2)	-0.91(-12)	0.44(- 3)	0.59(-11)
	00D1k	D_2CO	0.31(- 9)	0.14(-1)	-0.25(- 2)	-0.25(- 2)	-0.74(-10)	0.40(- 3)	0.41(-10)

[a] $00D1k = \langle \chi_{00}|D|\chi_{1k}\rangle$ (-6) means 10^{-6}

Table 4.6.

mode	integral[a]	k=						
H_2CO		0	1	2	3	4	5	6
1	0k10	0.98	-0.17	0.59(- 2)	0.77(-2)	-0.23(- 2)	-0.12(- 2)	0.14(- 2)
	0k11	0.17	0.96	-0.23	0.21(-1)	0.75(- 2)	-0.43(- 2)	0.35(- 4)
2	0k10	0.31	0.48	0.53	0.47	0.34	0.21	0.12
	0k11	-0.44	-0.41	-0.12	0.22	0.42	0.44	0.35
	0k12	0.48	0.16	-0.26	-0.36	-0.13	0.19	0.38
	0k13	-0.45	0.11	0.35	0.66(-1)	-0.28	-0.31	-0.62(- 1)
3	0k10	0.91	-0.39	0.12	-0.32(-1)	0.84(- 2)	0.85(- 3)	-0.25(- 2)
4	0k10	0.71	0.87(-4)	0.53	0.73(-3)	0.39	-0.95(- 3)	0.22
	0kD10	-0.20(- 5)	-0.54(-1)	-0.40(- 4)	-0.58(-1)	-0.11(- 3)	-0.44(- 1)	0.31(- 3)
	0k11	0.20(- 4)	0.62	0.39(- 3)	0.59	1.0 (- 3)	0.43	-0.30(- 2)
	0kD11	-0.23(- 1)	-0.15(-4)	-0.67(- 1)	-0.15(-3)	-0.71(- 1)	0.13(- 3)	-0.47(- 1)
	0k12	0.64	0.10(-3)	0.23	0.13(-2)	0.50	-0.32(- 3)	0.42
	0kD12	0.20(- 5)	0.13(-1)	-0.52(- 4)	-0.47(-1)	-0.26(- 3)	-0.68(- 1)	0.43(- 3)
	0k13	0.64(- 5)	-0.64	0.29(- 3)	0.67(-1)	0.32(- 2)	0.45	-0.26(- 2)
	0kD13	0.25(- 1)	-0.63(-5)	0.32(- 1)	-0.14(-3)	-0.36(- 1)	-0.17(- 3)	-0.69(- 1)
5	0k10	1.0	0.41(-7)	-0.93(- 2)	0.13(-7)	0.61(- 3)	0.28(- 9)	0.42(- 3)
	0kD10	-0.12(- 9)	-0.21(-1)	-0.11(- 8)	0.13(-3)	0.46(-11)	-0.10(- 3)	-0.19(-11)
	0k11	0.48(- 8)	1.0	0.53(- 7)	-0.12(-1)	0.23(-11)	0.25(- 2)	-0.38(-10)
	0kD11	-0.21(- 1)	-0.22(-9)	-0.28(- 1)	-0.53(-8)	-0.39(- 4)	-0.88(-11)	-0.19(- 3)
6	0k10	0.99	0.69(-7)	0.10	0.60(-7)	0.13(- 1)	0.65(-10)	0.16(- 2)
	0kD10	-0.59(-11)	0.18(-1)	0.60(-11)	0.32(-2)	0.15(-11)	0.48(- 3)	0.41(-11)
	0k11	0.36(- 9)	0.98	-0.20(- 6)	0.17	0.75(- 7)	0.27(- 1)	-0.28(- 7)
	0kD11	0.16(- 1)	0.13(-8)	0.27(- 1)	0.55(-8)	0.63(- 2)	0.16(- 8)	0.11(- 2)

[a] $0kD10 = \langle \chi_{0k} | D | \chi_{10} \rangle$ (-6) means 10^{-6}

polarizations agree with the experimental ones.

The hot bands in H_2CO are obtained from Table 4.6:

$1_1^{0*}\ 1_1^{1*}$	(B or C polarization)	
$2_1^0\ 2_1^{1*}$	("	")
3_1^{0*}	("	")
4_1^0	(B	")
$4_1^{1*}\ 4_1^{3*}$	(C	")
$4_2^1\ 4_2^{3*}$	(B	")
4_2^{0*}	(C	")
5_1^{0*}	(C	")
6_1^0	(C	")

The asterisk-marked progressions are experimentally not found, while the others are found; all polarizations agree with the experimental ones. The hot bands from modes 1 and 5 are not seen experimentally, because the first excited level in these modes has a rather high energy (3000 cm^{-1}). There is one experimental progression that is not found in the calculation: 4_1^2.

This one occurs in the combination assigned $3_0^1 4_1^2$ at 28450 cm^{-1} with B polarization. For the $3_0^1 4_1^0$ band the calculated intensity is 17 times that of the $3_0^1 4_1^2$ transition (see Table 4.7.) as was already alluded to on p.**66**; with the revised value for ν_3 the progression does not occur in H_2CO. For D_2CO the 4_1^2 progression is 2.5 times stronger than for H_2CO and for D_2CO it has experimentally been observed as 4_1^2 (see Table 4.7.).

In Table 4.7. the calculated oscillator strengths are shown for all observed bands in H_2CO and also for the bands involving mode 3, using 1428 cm^{-1} for ν_3. One can see again that it is extremely unlikely that the $3_0^1 4_1^2$ hot band can be observed in the spectrum, noting the large oscillator strengths apparently necessary to observe a band in the hot spectrum at all.

One expects that the $2_0^1 3_0^1 4_0^1$ transition can be seen in the experimental spectrum, because it does not lie on the flank of a strong transition. It will be interesting to

Table 4.7.

transition	ΔE (cm^{-1})	D	f	polarization
H_2CO				
cold				
4_0^1	28312	0.629 (-2)	3.41 (-6)	B
4_0^3	29136	0.684 (-2)	4.15 (-6)	B
$2_0^1 4_0^1$	29495	0.893 (-2)	7.15 (-6)	B
$4_0^2 6_0^1$	29634	0.283 (-2)	0.72 (-6)	C
$3_0^1 4_0^1$*	29742	0.276 (-2)	0.69 (-6)	B
$2_0^1 4_0^3$	30340	0.971 (-2)	8.72 (-6)	B
$3_0^1 4_0^3$*	30565	0.301 (-2)	0.84 (-6)	B
$2_0^2 4_0^1$	30659	0.974 (-2)	8.85 (-6)	B
$2_0^1 4_0^2 6_0^1$	30819	0.402 (-2)	1.51 (-6)	C
$2_0^1 3_0^1 4_0^1$*	30914	0.392 (-2)	1.45 (-6)	B
5_0^1	31156	0.408 (-2)	1.58 (-6)	C
$1_0^1 4_0^1$	31159	0.109 (-2)	0.12 (-6)	B
$2_0^2 4_0^3$	31531	1.059 (-2)	10.42 (-6)	B
$2_0^1 3_0^1 4_0^3$*	31738	0.427 (-2)	1.76 (-6)	B
$2_0^3 4_0^1$	31809	0.913 (-2)	8.07 (-6)	B
$1_0^1 4_0^3$	31987	0.112 (-2)	0.12 (-6)	B
$2_0^1 5_0^1$	32335	0.579 (-2)	3.31 (-6)	C
$2_0^6 4_0^1$	35090	0.386 (-2)	1.59 (-6)	B
$1_0^1 2_0^4 4_0^3$	35740	0.142 (-2)	0.22 (-6)	B
$2_0^6 4_0^3$	36220	0.419 (-2)	1.94 (-6)	B
$1_0^1 2_0^5 4_0^1$	37250	0.099 (-2)	0.11 (-6)	B
hot				
$3_0^1 4_1^2$	28450	0.156 (-2)	0.21 (-6)	B
$3_0^1 4_1^1$	28450	0.648 (-2)	3.64 (-6)	B
4_1^2*	27563	0.355 (-2)	1.06 (-6)	B
$2_0^1 4_1^2$	27241	2.601 (-2)	56.12 (-6)	B
4_1^0	27021	1.48 (-2)	17.94 (-6)	B
$2_0^0 4_1^1$	26567	0.97 (-2)	7.61 (-6)	B
4_2^1	26061	1.83 (-2)	26.63 (-6)	B
D_2CO				
hot				
4_1^2	27753	0.561 (-2)	2.65 (-6)	B

(-6) means 10^{-6}

*)Not observed in the experimental spectrum.

see further experimental material in this respect and also
regarding the intensities, as no experimental spectrum has
been published so far, in which the intensities of the
different transitions are shown.

4.2. The $^1A_1$-$^1A_2$ Non-Radiative Transition

In principle, the coupling of each vibrational level
of the $^1A_2$ state with each vibrational level of the $^1A_1$
state consists of 84 terms:

a) The coupling in Q_0, consisting of 12 components, being
   the derivatives in 12 directions.
b) The coupling as a result of the 6 normal modes; each
   normal mode coupling has 12 components, being the deri-
   vative of Q in 12 directions.

It is possible to derive from symmetry considerations
which components of the electronic coupling element be-
tween the $^1A_1$ and $^1A_2$ state are unequal zero[8]. The symmetry
of the 6 vibrational normal modes and of the rotations and
translations are shown below:

mode	kind	symmetry
1	vibrat.	A_1
2	"	A_1
3	"	A_1
4	"	B_1
5	"	B_2
6	"	B_2
7	R_x	A_2
8	R_y	B_1
9	R_z	B_2
10	X	A_1
11	Y	B_2
12	Z	B_1

For mode 4 (B_1 symmetry) we have contributions[*] of B_2 symmetry: $\dfrac{\partial}{\partial Q_5}$, $\dfrac{\partial}{\partial Q_6}$, $\dfrac{\partial}{\partial R_z}$, $\dfrac{\partial}{\partial y}$

For mode 5 (B_2 symmetry) we have contributions of B_1 symmetry: $\dfrac{\partial}{\partial Q_4}$, $\dfrac{\partial}{\partial R_y}$, $\dfrac{\partial}{\partial z}$

For mode 6 (B_2 symmetry) we have contributions of B_1 symmetry: $\dfrac{\partial}{\partial Q_4}$, $\dfrac{\partial}{\partial R_y}$, $\dfrac{\partial}{\partial z}$

$\dfrac{\partial}{\partial R_x}$ has A_2 symmetry, therefore this component of the coupling has a contribution in all modes and Q_0.

In other words:

coordinate Q_4 has electronic coupling component 5, 6, 9 and 11 unequal zero,

coordinate Q_5 has electronic coupling component 4, 8 and 12 unequal zero,

coordinate Q_6 has electronic coupling component 4, 8 and 12 unequal zero,

all coordinates have electronic coupling component 7 unequal zero.

This is exactly what is found the *ab initio* CI calculations; the resulting coupling terms are shown in Figure 4.3.

We next calculate which vibrational levels of the ground state lie in an interval ΔE around a vibrational level of the excited state. The energy of the excited state level (see eq. (3.47)) was calculated with for $\Phi_1(Q_0)-\Phi_0(Q_0)$ the experimental value (the experimental value is 3430.6 cm^{-1} larger than the calculated one, see Chapter 4.1.); if the theoretical value is used, the results below are virtually unaltered.

---

[*] $\left\langle \phi_0(Q_e) \middle| \dfrac{\partial}{\partial Q_j} \middle| \phi_1(Q_e) \right\rangle_e$ has to contain the A_1 representation.
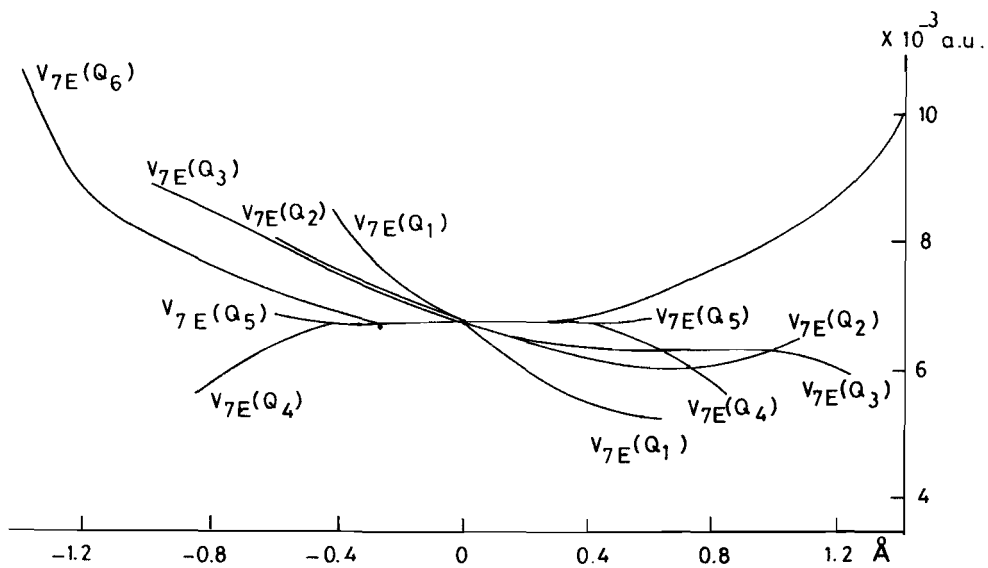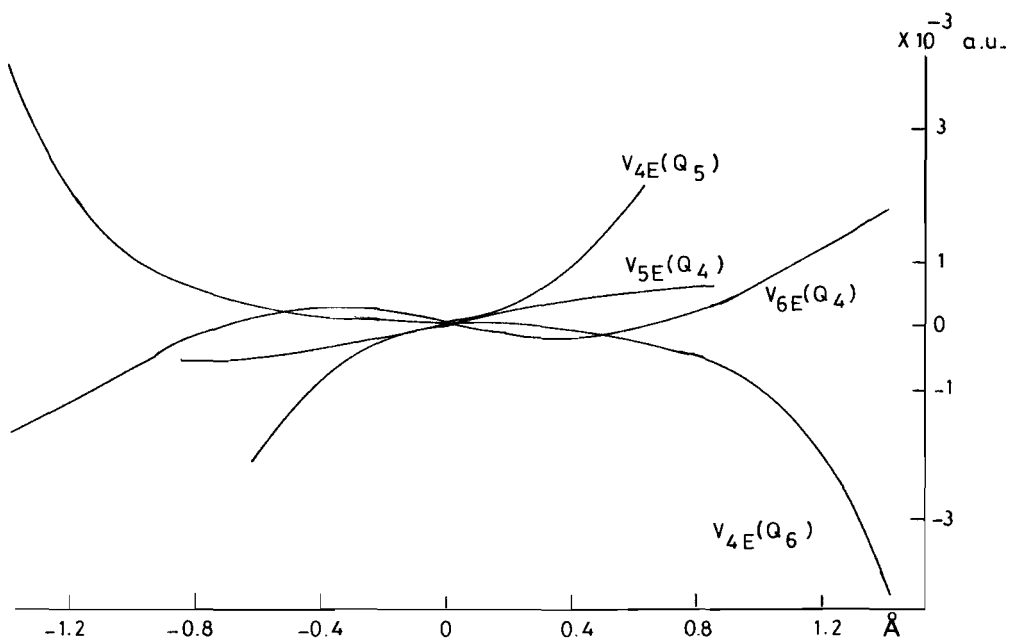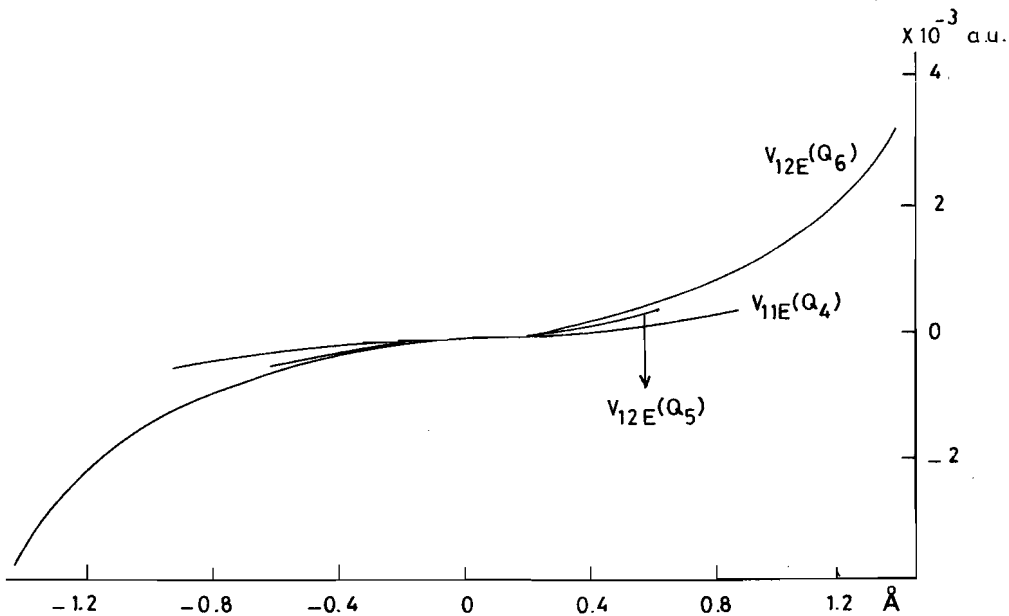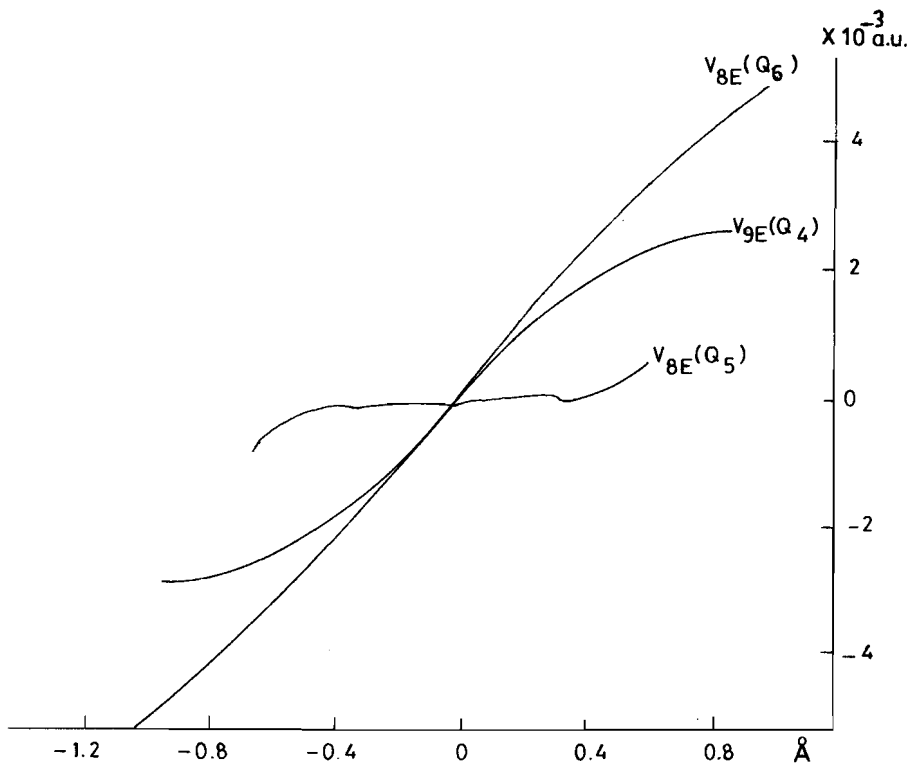
Fig. 4.3. a)

Fig. 4.3. b)

The raw level density varies from 10 per cm^{-1} around the 4^1 level, to 18 per cm^{-1} for the $2^1 5^1$ level. The largest couplings that occur are 5.10^{-6} a.u., the smallest are 10^{-23} a.u. Couplings smaller than 10^{-7} have a negligable effect upon the oscillator strength distribution and the time evolution thereof. It turns out that if ΔE is taken larger than 10 cm^{-1}, no appreciable difference in the oscillator profile occurs, when compared with the $\Delta E = 10$ cm^{-1} case. The number of levels with a coupling larger than 10^{-7} is extremely low, varying from 0 to 6 with an average of 3. No clear dependence on energy or type of excited level can be observed, neither are the S_0 levels that have the largest couplings, of a particular type. Calculation of the energy function $P_1(t)$ (see eq. (3.58); all levels in the $\Delta E = 10$ cm^{-1} are excited) results for all excited state levels in an oscillatory behaviour of the oscillator strength, with oscillating times varying from $2. \ 10^{-12}$ to $2. \ 10^{-10}$ sec. In other words, in H_2CO (and also D_2CO, see below) we have an example of the so-called resonance case[17]. In the resonance case the density of coupling levels is so low, that any interaction depends on the fortuitous position of the interacting levels. In D_2CO the raw density is about two times of that of H_2CO at the same S_1 level. The couplings are, however, a factor 10 smaller, so that here even fewer levels effectively couple with the excited state levels.
It is seen from Figure 4.3. that there is also rotational coupling between the S_1 and S_0 states. This means that for rotation states with at least one quantum number unequal zero, there is an extra coupling. The R_x component will give the main contribution, because it is unequal zero in Q_0.
The rotational wave function for a rigid symmetric top molecule (formaldehyde is well described by this, as it is an almost symmetric top molecule) is:

$$\mathcal{R}_{JK}(\theta, \varphi) = \mathcal{Y}_{JK}(\theta, \varphi) = P_J^{|K|}(\theta, \varphi) \cdot e^{-iK\varphi} \qquad (4.1)$$

$$\mathcal{Y} = \text{spherical harmonic}$$

$$P = \text{associated Legendre polynomial}$$

Therefore:
$$\frac{\partial}{\partial \varphi} \mathcal{R}_{JK} = -iK \cdot \mathcal{R}_{JK} \qquad (4.2)$$

So the rotational coupling depends linearly on K (see also eq. (2.36) . However, inclusion of the rotational coupling does not alter the resonance behaviour of the S_1 levels; even for K = 10 there are added only a couple of levels to the ones originating from the vibrational components. It should be noted that a certain rotational state of S_1 couples only with the same rotational state of S_0, because of the orthogonality of the rotational states.

From Figure 4.3. it is also seen that there are translational components in the non-adiabatic coupling between S_1 and S_0. It should be noted that the $\frac{\partial}{\partial R}$ is taken with respect to electron coordinates held fixed in the center of mass of the nuclei coordinate system; this approximation is not valid anymore when the translational velocity of the nuclei is appreciable with respect to the internal velocity of the electrons[27].

We take for the translation function a plane wave in the x-direction:

$$T(x,t) = A \cdot e^{-i(kx - \omega t)} \qquad (4.3)$$

The translation energy E = ω.

k is the propagation vector: k = p, with p, the translational momentum of the molecule; M is the mass of the molecule.

So:
$$k = \sqrt{2M \cdot E} \qquad (4.4)$$

We obtain:
$$\frac{\partial}{\partial g_T} T(x,t) = \frac{-ik}{\sqrt{M}} \cdot T(x,t) = -i\sqrt{2E} \cdot T(x,t) \qquad (4.5)$$

$$\text{with } g_T = \sqrt{M} \cdot x \quad (\text{see eq. (4.3)})$$

This result is not changed if we form a wave packet, be-
cause the wave packet will only contain plane waves which
have about the same k.
So the translational component of the non-adiabatic coup-
ling is linearly dependent on the translational momentum
of the molecule. The translational energy available to one
coordinate is approximately $\frac{1}{2}$k.T, k = Boltzmanns constant,
T is the absolute temperature.
For T = 296 ^{O}K we obtain:
$\frac{1}{2}$k.T = 4.6 10^{-4} a.u.
So the translational components of the coupling are multi-
plicated with 4.6 10^{-4} at 23 ^{O}C. Of course the translation-
al components should actually be identical to zero; the
deviation from zero indicates the error made by keeping
the electron coordinates fixed while differentiating.

The accuracy of the non-adiabatic coupling elements can be
estimated by comparing the length and acceleration dipole
transition moments for the $S_0 \rightarrow S_1$ transition (see p. **68**).
It was estimated there that the coupling elements are
possibly a factor 3-80 too large. It is obvious that this
does not afflict any of the conclusions about the internal
conversion in formaldehyde.

The exponential radiationless decays observed in formal-
dehyde[4-7] have lifetimes varying from $5 \cdot 10^{-9}$ to $8 \cdot 10^{-8}$ sec.
Clearly, these processes cannot be explained by internal
conversion as the calculations show. We can explain the
exponential decay by considering the coupling between the
S_1 levels and the dissociative continuum states of S_0.
Formaldehyde can give two reactions:

H_2CO (S_1) $\rightarrow$ H_2 + CO   (1) ΔE -140 cm^{-1}
                $\rightarrow$ H + HCO   (2) ΔE 32000 cm^{-1}
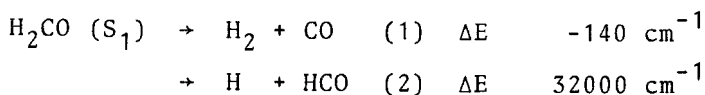
The quantum yield for dissociation of formaldehyde is
0.96-1.0. Process (1) predominates for energies near the
S_1 origin at 28188 cm^{-1}, process (2) predominates for

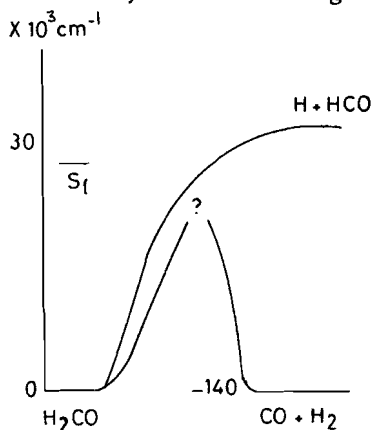energies above 32250 cm^{-1} [18]. The potential energy surface is schematically drawn in Figure 4.4.

Fig. 4.4.

The barrier height for reaction (1) is unknown. We assume that the barrier is below the S_1 state, as is also corroborated by our calculations on mode 1 (see Figure 4.1.). The time evolution of the system can now be described if we know the complete set of eigenfunctions and the state at t = 0. We will consider the case of one discrete state ψ_1 interacting with two continua $\zeta_{E'}$ and $\eta_{E'}$; the case of n continua can be obtained by simple extension. H being the total Hamiltonian, we assume that the interaction matrix has the form:

$$\langle \psi_1 \,/\, H \,/\, \psi_1 \rangle = E_1$$
$$\langle \zeta_{E'} \,/\, H \,/\, \psi_1 \rangle = V_{E'}$$
$$\langle \eta_{E'} \,/\, H \,/\, \psi_1 \rangle = W_{E'} \tag{4.6}$$
$$\langle \zeta_{E''} \,/\, H \,/\, \zeta_{E'} \rangle = \langle \eta_{E''} \,/\, H \,/\, \eta_{E'} \rangle = E' \, \delta(E'' = E')$$
$$\langle \zeta_{E''} \,/\, H \,/\, \eta_{E'} \rangle = 0$$

The eigenvectors to be determined have the form:

$$\overline{\Psi}_{\lambda E} = a \, \psi_1 + \int [\, b_{E'} \, \zeta_{E'} + c_{E'} \, \eta_{E'} \,] \, dE' \tag{4.7}$$

h is required to completely specify ψ, since each value of
E is twofold degenerate.

Fano[26] has solved this problem. For the moment we are only
interested in a. Of the two solutions that are obtained,
one has a = 0, the other one has:

$$|a(E)|^2 = \frac{|V_E|^2 + |W_E|^2}{[E - E_1 - G(E)]^2 + \pi^2(|V_E|^2 + |W_E|^2)^2}$$

$$\text{With } G(E) = P \int dE' \frac{|V_{E'}|^2 + |W_{E'}|^2}{E - E'}$$

$$P \text{ denotes the "principal part of"}$$

This is a resonance curve (Lorenzian for constant V and W)
with its center at the zero point of $E - E_1 - G(E)$, and
half width $\pi(|V_E|^2 + |W_E|^2)$ If at t = 0 the system is pre-
pared in the state ψ_1, the state will decay with a mean
life time of:

$$[2\pi(|V_E|^2 + |W_E|^2)]^{-1}$$

If besides ψ_1 also one or more continua have oscillator
strength, the absorption peak becomes asymmetric as des-
cribed by Fano; it would be interesting to see if this be-
haviour can be observed in formaldehyde.

We observe that the coupling of S_1 with the continuum ex-
plains the exponential decay of the S_1 levels; the eva-
luation of the coupling with the continua will have to
await further research.

For the 4^1 level in D_2CO it is experimentally observed
that the quantum yield for dissociation is 0.0[28]; the
radiationless lifetime $\tau_{NR} \geqslant 45$ μsec., about a factor 500
larger than the corresponding H_2CO level. If the previous-
ly noted ratio of 10 for the H_2CO and D_2CO coupling con-

tinues into the continuum, this explains the two orders of magnitude longer lifetime of the D_2CO levels and the corresponding zero dissociation yield.

4.3. Comparing the Adiabatic and Crude Adiabatic Results

The energies of the S_0 and S_1 state of formaldehyde were calculated as a function of the six normal coordinates. Two of the resulting 0-1 vibrational frequencies are shown in Table 4.8., where they are compared with experiment. It is observed that these results are much too high; this is in agreement with an earlier calculation of Atabek[12] on H_2 and N_2.

Table 4.8.

mode	$^1A_1$		$^1A_2$	
mode	calcul.	exper.	calcul.	exper.
1	18727	2766.4	20367	2847
6	49408	1251.2	49395	904

The CBO set cannot be used to calculate the internal conversion in formaldehyde, because:
1) The potential energy curves do not resemble the experimental ones: in mode 6 the calculated 0-1 IR transition has an energy higher than the observed $S_0 \rightarrow S_1$ UV transition.
2) The coupling between S_0 and S_1 is zero, because of symmetry reasons.

So comparing the ABO and CBO results we find that the former are clearly superior for describing the radiationless process in formaldehyde.
We can now also check to what extent the inequality (1.35) is satisfied by the two basis sets.

From Table 4.4. we see that for the ABO set ΔE is minimally of the order of 100 cm^{-1} = $5 \cdot 10^{-4}$ a.u. From Chapter 4.2. we know that $\nu \simeq 10^{-6}$ a.u., and $\varepsilon \simeq 3$ cm^{-1} $\simeq 10^{-5}$ a.u. From Chapter 4.1. we can calculate that $\tau_r \simeq 1$ μ sec.; this corresponds to a $\Gamma_r \simeq 10^{-11}$ a.u. So substituting these values in the inequality (1.35) we obtain:

$$5 \cdot 10^{-4} \gg 3 \cdot 10^{-11} + 3 \cdot 10^{-7} + 2 \cdot 10^{-6}$$

So inequality (1.35) is satisfied for the ABO set.

For the CBO set $\nu = 0$ and also $\Gamma_r = 0$, because with the CBO set one calculates probability zero for exciting the $^1A_2$ state. The ΔE is roughly a factor 10 larger than for the ABO set, so ΔE 5.10^{-3} a.u. So we obtain:

$$5 \cdot 10^{-3} \gg 0 + 0 + 0$$

Obviously the inequality is also satisfied for the CBO set. Inequality (1.35) is derived from condition II. It appears from the results that for formaldehyde condition I is a stronger condition than condition II. As the couplings with the higher states were not calculated, it is not possible to check condition I.

84

The set of equations (1.30) is identical to the set of
equations that appears in a paper of Bixon and Jortner[2].
They derive that:

$$a_{l,l}^2 = \frac{\mathcal{N}^2}{(E - E_{l,l})^2 + \left(\frac{\pi \mathcal{N}^2}{\epsilon}\right)^2} \qquad (A.1)$$

and

$$a_{ok} = \frac{-\mathcal{N} \cdot a_{ll}}{E_{ok} - E} \qquad (A.2)$$

So:

$$\mathcal{N} \sum_k a_{ok} = \mathcal{N}^2 a_{ll} \sum_k \frac{1}{E - E_{ok}} =$$

$$= \frac{\mathcal{N}^3}{\left[(E - E_{ll})^2 + \left(\frac{\pi \mathcal{N}^2}{\epsilon}\right)^2\right]^{\frac{1}{2}}} \cdot \sum_k \frac{1}{E - E_{ok}} \qquad (A.3)$$

Also from reference 2:

$$\mathcal{N}^2 \sum_k \frac{1}{E - E_{ok}} = E_{ll} - E \qquad (A.4)$$

So:

$$\mathcal{N} \sum_k a_{ok} = \frac{\mathcal{N} (E_{ll} - E)}{\left[(E_{ll} - E)^2 + \left(\frac{\pi \mathcal{N}^2}{\epsilon}\right)^2\right]^{\frac{1}{2}}} \qquad (A.5)$$

We consider:[12-15]

$$0 = \frac{\partial}{\partial \vartheta} \frac{\partial}{\partial \vartheta} \cdot \langle a \mid b \rangle$$

$$= \frac{\partial}{\partial \vartheta} \left\{ \langle \frac{\partial a}{\partial \vartheta} \mid b \rangle + \langle a \mid \frac{\partial b}{\partial \vartheta} \rangle \right\} \qquad (A.6)$$

$$= \frac{\partial}{\partial \vartheta} \left\{ -\langle a \mid \frac{\partial}{\partial \vartheta} \mid b \rangle \right\} + \langle \frac{\partial a}{\partial \vartheta} \mid \frac{\partial b}{\partial \vartheta} \rangle + \langle a \mid \frac{\partial^2 b}{\partial \vartheta^2} \rangle$$

Inserting in the second term the unity operator $1 = \sum_P |p \rangle\langle p|$ (the set $|p\rangle$ being complete) we obtain:

$$\langle a \mid \frac{\partial^2}{\partial \vartheta^2} \mid b \rangle = \frac{\partial}{\partial \vartheta} \left\{ \langle a \mid \frac{\partial}{\partial \vartheta} \mid b \rangle \right\} - \sum_P \langle \frac{\partial a}{\partial \vartheta} \mid p \rangle\langle p \mid \frac{\partial b}{\partial \vartheta} \rangle$$

$$\qquad (A.7)$$

$$= \frac{\partial}{\partial \vartheta} \left\{ \langle a \mid \frac{\partial}{\partial \vartheta} \mid b \rangle \right\} + \sum_P \langle a \mid \frac{\partial}{\partial \vartheta} \mid p \rangle\langle p \mid \frac{\partial}{\partial \vartheta} \mid b \rangle$$

A straightforward but long and tedious derivation[11] gives:

$$\langle \phi_1' \,|\, \frac{\partial^2}{\partial \vartheta_k^2} \,|\, \phi_0 \rangle_{\ell} = \frac{2}{(\bar{E}_0 - \bar{E}_1)^2} \langle \phi_1 \,|\, \left(\frac{\partial u}{\partial \vartheta}\right)^2 |\, \phi_0 \rangle_{\ell} +$$

$$- \frac{4}{(\bar{E}_0 - \bar{E}_1)^2} \; \frac{\partial \bar{E}_0}{\partial \vartheta_k} \cdot \langle \phi_1 \,|\, \frac{\partial u}{\partial \vartheta_k} |\, \phi_0 \rangle_{\ell} + \qquad (A.8)$$

$$+ \frac{1}{(\bar{E}_0 - \bar{E}_1)} \cdot \langle \phi_1 \,|\, \frac{\partial^2 u}{\partial \vartheta_k^2} |\, \phi_0 \rangle_{\ell}$$

$\langle \phi_1 \,|\, \frac{\partial u}{\partial \vartheta_k} |\, \phi_0 \rangle_{\ell}$ can be calculated *via* the methods of Chapter 2 (see (2.16)).

$\langle \phi_1 \,|\, \frac{\partial^2 u}{\partial \vartheta_k^2} |\, \phi_0 \rangle_{\ell}$ can be calculated with the field-gradient operator (9 components per atom!).

$\langle \phi_1 \,|\, \left(\frac{\partial u}{\partial \vartheta_k}\right)^2 |\, \phi_0 \rangle_{\ell}$ cannot be calculated with a standard properties program.

APPENDIX 4 (see p.23)

Using eq. (1.21): $\quad \left(H_0 - \mathcal{E}_0(Q) \right) \phi_0(q, Q) = 0 \qquad$ (A.9)

we obtain: $\langle \phi_1 \,|\, \frac{\partial}{\partial Q} \,|\, \phi_0 \rangle_q = \langle \phi_1 \,|\, \frac{\partial}{\partial Q} \,|\, \frac{H_0}{\mathcal{E}_0(Q)} \cdot \phi_0 \rangle_q =$

$$= \langle \phi_1 \,|\, \frac{H_0}{\mathcal{E}_0(Q)} \frac{\partial}{\partial Q} \,|\, \phi_0 \rangle_q + \langle \phi_1 \,|\, \{ \frac{\partial}{\partial Q} \frac{H_0}{\mathcal{E}_0(Q)} \} \,|\, \phi_0 \rangle_q$$

(A.10)

$$= \frac{\mathcal{E}_1(Q)}{\mathcal{E}_0(Q)} \langle \phi_1 \,|\, \frac{\partial}{\partial Q} \,|\, \phi_0 \rangle_q +$$

$$+ \langle \phi_1 \,|\, \frac{1}{\mathcal{E}_0(Q)^2} \{ \mathcal{E}_0(Q) \frac{\partial H_0}{\partial Q} + H_0 \cdot \frac{\partial \mathcal{E}_0(Q)}{\partial Q} \} \,|\, \phi_0 \rangle_q$$

Now $\frac{\partial H_0}{\partial Q} = \frac{\partial U}{\partial Q}$, in which U represents the potential energy terms. The term with $\frac{\partial \mathcal{E}_0(Q)}{\partial Q}$ does not contribute, because of the orthogonality of ϕ_1 and ϕ_1.

So we obtain:

$$\langle \phi_1 \,|\, \frac{\partial}{\partial Q} \,|\, \phi_0 \rangle_q = \frac{\langle \phi_1 \,|\, \frac{\partial U}{\partial Q} \,|\, \phi_0 \rangle_q}{\mathcal{E}_0(Q) - \mathcal{E}_1(Q)} \qquad (A.11)$$

REFERENCES

Chapter 0

1. S.J. Strickler, R.A. Berg, J. Chem. Phys. 48 (68) 715
2. S.J. Strickler, J.P. Vikesland, H.D. Bier, J. Chem. Phys. 60 (74) 664
3. N. Mataga, J. Koluta,"Molecular Interactions and Electronic Spectra" (Marcel Dekker, New York, 1970)
4. M. Bixon, J. Jortner, J. Chem. Phys. 48 (68) 715
5. S.H. Lin, Proc. Roy. Soc. Lond. A 352 (76) 57

Chapter 1

1. R. Voltz, Symposium on Radiationless Processes (Breukelen, Holland, 1977)
2. M. Bixon, J. Jortner, J. Chem. Phys. 48 (68) 715
3. J. Jortner, R.S. Berry, J. Chem. Phys. 48 (68) 2757
4. M. Born, K. Huang, "Dynamical Theory of Crystal Lattices" (Oxford 1954), p. 406

Chapter 2

1. M. Bixon, J. Jortner, J. Chem. Phys. 48 (68) 715
2. W.M. Gelbart, D.F. Heller, M.L. Elert, Chem. Phys. 7 (75) 116
3. C. Tric, Chem. Phys. Lett. 21 (73) 83
4. F. Lahmani, A. Tramer, C. Tric, J. Chem. Phys. 60 (74) 4431
5. J.M. Delory, C. Tric, Chem. Phys. 3 (74) 54
6. C.A. Langhoff, G.W. Robinson, Mol. Phys. 26 (73) 249
7. R.A. van Santen, Thesis (Leiden, 1971)
8. M. Roche, H.H. Jaffé, Chem. Rev. 5, 165
9. P. Gans, "Vibrating Molecules" (Chapman & Hall, 1971)
10. E.B. Wilson, J.C. Decius, P.C. Cross, "Molecular Vibrations" (McGraw Hill, 1955)
11. M.J.H. Kemper, Afstudeerverslag (Eindhoven University of Technology, Eindhoven, The Netherlands, 1976)

12. V. Sidis, Lefebre-Brioullion, J. Phys. B. 1971, 1040
13. See ref. 27 of Chapter 4
14. J.C. Browne in "Energy, Structure and Reactivity" (Ed. D.W. Smith, W.B. McRae, Wiley, 1973) p. 2
15. J.C. Tully in "Molecular Collisions" (Ed. W.H. Miller, Plenum Press 1976), Part B, p. 231

Chapter 3

1. J.L. Duncan, P.D. Mallinson, Chem. Phys. Lett. 23 (73) 597
2. R.C. Weast ed., "Handbook of Chemistry and Physics" (CRC Press 56th edit.), p. B-253
3. These are the Schachtscheider programs, kindly provided by dr. D.L. Vogel and ir. J.P. Bronseijk
4. T.H. Dunning, J. Chem. Phys. 53 (70) 2823
5. The IBMOL 5,H program was written by dr. E. Clementi; the four-index-transformation program was written by dr. M. van Hemert; the properties program of POLYATOM was written by D. Neumann. We thank dr. P.E.S. Wormer of Nijmegen University for making available these programs.
6. R.J. Buenker, S.D. Peyerimhoff, J. Chem. Phys. 53 (70) 1368
7. H.F. Schaefer III in "Energy, Structure and Reactivity", ed. by D.W. Smith and W.B. McRae (Wiley Interscience 1973) p. 158
8. V. Fock, Z. Physik 61 (30) 126
9. J.C. Slater, Phys. Rev. 35 (30) 210
10. D.R. Hartree, Proc. Cambridge Phil. Soc. 24 (28) 89
11. C.C.J. Roothaan, Rev. Mod. Phys. 23 (51) 69
12. D.B. Cook, "*Ab Initio* Valence Calculations in Chemistry" (Buttersworth 1974) p. 137, 95
13. O. Goscinski, B.T. Pickup, G. Purvis, Chem. Phys. Lett. 22 (73) 167
14. O. Goscinski, G. Howat, T. Aberg, J. Phys. B. 8 (75) 11

15. G. Howat, O. Goscinski, T. Aberg, Physsica Fennica 1974, p. 241

16. G. Howat, O. Goscinski, Chem. Phys. Lett. 30 (75) 87

17. O. Goscinski, B.T. Pickup, Chem. Phys. Lett. 33 (75) 265

18. O. Goscinski, M. Hehenberger, B. Roos, P. Siegbahn, Chem. Phys. Lett. 33 (75) 427

19. O. Goscinski, Int. J. Quant. Chem. (Symp.) 9 (75) 221

20. K. Morokuma, H. Konishi, J. Chem. Phys. 55 (71) 402

21. D.M. Hayes, K. Morokuma, Chem. Phys. Lett. 12 (72) 539

22. S. Ehrenson, P.E. Phillipson, J. Chem. Phys. 34 (61) 1224

23. TRAPRB, a computer program for molecular transitions by W.R. Jarmain and J.C. McCallum, University of Western Ontario, Department of Physics, 1970. We thank the authors for sending us the program.

24. W.R. Jarmain, J. Quant. Spectrosc. Radiat. Transfer, 11 (71) 421

25. W.R. Jarmain, J. Quant. Spectrosc. Radiat. Transfer, 12 (72) 603

26. R.N. Zare, J.K. Cashion, UCRL (University of California, Lawrence Radiation Laboratory) 10881 (1963)

27. J.W. Cooley, Math. Comp. 15 (61) 363

28. D.R. Hartree, "Numerical Analysis" (Claridon Press, Oxford 1952)

29. M.J.H. Kemper, J.M.F. van Dijk, H.M. Buck, Chem. Phys. Lett., to be published

30. D.H. Lehmer in "Applied Combinatorial Mathematics". Ed. E.F. Beckenbach (Wiley, New York, 1964)

31. D.M. Burland, G.W. Robinson, J. Chem. Phys. 51 (69) 4548

32. P.C. Haarhoff, Mol. Phys. 7 (63) 101

33. H. Kiesewetter, G. Maess, "Elementare Methoden der Numerische Mathematik" (Springer Verlag, New York) p. 220

34. R. Wallace, Chem. Phys. 11 (75) 189

35. Personal communication, ir. W.A.M. Castenmiller

36. B.R. Henry, W. Siebrand, J. Chem. Phys. 49 (68) 5369

37. R.J. Hayward, B.R. Henry, J. Molec. Spectrosc. 46 (73) 207

38. R.J. Hayward, B.R. Henry, Chem. Phys. 12 (76) 387

39. F.L. Pilar, "Elementary Quantum Chemistry" (McGraw Hill 1968)

40. J.L. Duncan, P.D. Mallinson, Chem. Phys. Lett. 23 (73) 597

41. V.T. Jones, J.B. Coon, J. Mol. Spectr. 31 (69) 137

42. B. Numerov, Publ. de l'Observ. Astrophysique Centrale de Russie 2 (33) 188

43. A.M. Donner, M.W. Holtrop, H. Peschar, "Rapport van de Commissie van Drie" (Staatsuitgeverij, Den Haag, 1976), p. 13

44. E.S. Yeung, C.B. Moore, J. Chem. Phys 58 (73) 3988

45. E.S. Yeung, C.B. Moore, J. Che,. Phys. 60 (74) 2139

46. A.C. Luntz, V.T. Maxson, Chem. Phys. Lett. 26 (74) 553

47. K.Y. Tang, P.W. Fairchild, E.C. Lee, J. Chem. Phys. 66 (77) 3303

Chapter 4

1. D.C. Moule, A.D. Walsh, Chem. Rev. 75 (75) 67

2. J.L. Duncan, P.D. Mallinson, Chem. Phys. Lett. 23 (73) 597

3. V.T. Jones, J.B. Coon, J. Mol. Spectr. 31 (69) 137

4. R.G. Miller, K.C. Lee, Chem. Phys. Lett. 33 (75) 104

5. R.G. Miller, K.C. Lee, Chem. Phys. Lett. 41 (76) 52

6. K.Y. Tang, E.K.C. Lee, Chem. Phys. Lett. 43 (76) 232

7. E.S. Yeung, C.B. Moore, J. Chem. Phys. 58 (73) 3988

8. E.S. Yeung, C.B. Moore, J. Chem. Phys. 60 (74) 2139

9. J.A. Pople, J.W. Sidman, J. Chem. Phys. 27 (57) 1270

10. K. Vasudevan, S.D. Peyerimhoff, R.J. Buenker, W.E. Kramer, Chem. Phys. 7 (75) 187

11. M. Peric, R.J. Buenker, S.D. Peyerimhoff, Can. J. Chem. 55 (77) 1533

12. O. Atabek, A. Hardisson, R. Lefebre, Chem. Phys. Lett. 20 (73) 40
13. J.M. Schoolery, A.H. Sharbaugh, Phys. Rev. 82 (51) 95
14. D.E. Freeman, W. Klemperer, J. Chem. Phys. 45 (66) 52
15. V.A. Job, V. Sethuraman, K.K. Innes, J. Mol. Spectr. 30 (69) 365
16. See ref. 3
17. J. Jortner, R.S. Berry, J. Chem. Phys. 48 (68) 2757
18. R.D. McQuigg, J.B. Calvert, J. Am. Chem. Soc. 91 (69) 1590
19. V. Sethuraman, V.A. Job, K.K. Innes, J. Mol. Spectr. 33 (70) 189
20. S. Chandrasekhar, Astrophys. J. 102 (45) 223
21. S. Ehrenson, P.E. Phillipson, J. Chem. Phys. 34 (61) 1224
22. A.W. Weiss, Astrophys. J. 138 (63) 1262
23. B. Schiff, C.L. Pekeris, Phys.Rev. 134 (64) A 638
24. H.A. Bethe, E.E. Salpeter, "Quantum Mechanics of One- and Two-Electron Atoms" (Academic Press, New York, 1957), p. 251-3
25. D.B. Neumann, J.W. Moskowitz, J. Chem. Phys. 50 (69) 2216
26. U. Fano, Phys. Rev. 124 (61) 1866
27. J.C. Browne in "Advances in Atomic and Molecular Physics", Ed. D.R. Bates and I. Esterman, Vol. 7 (71) 77 (Academic Press, New York)
28. R.G. Miller, E.K.C. Lee, Chem. Phys. Lett. 41 (76) 52
29. A.P. Baronavski, A. Hartford, C.B. Moore, J. Mol. Spectr. 60 (76) 111

SUMMARY

In Chapter 1 it is examined which conditions a basis
set must satisfy in order to describe radiationless decay.
These conditions are derived by examining which conditions
must be imposed on the exact equations for the process, in
order that they simplify to a generalized form of the
Bixon-Jortner model for radiationless decay.
In the remaining chapters the *ab initio* calculation of the
$S_1 \rightarrow S_0$ radiative and radiationless transition in formalde-
hyde is described. The calculation of the radiationless
process in formaldehyde was done with two basis sets: the
Adiabatic Born-Oppenheimer basis set and the Crude Born-
Oppenheimer basis set. The coupling in the ABO set was
calculated by expressing the coupling in integrals over
the electric field operator. The six-dimensional potential
energy surface for the nuclear movement was approximated
by six sections along the normal coordinates. The electronic
wave function was calculated with a Gaussian Atomic Orbital
set of double-zeta quality. The SCF MO's were calculated
with a modified Hartree-Fock operator: the Transition
operator; this ensures that the ground and $(n\pi^*)$ excited
state are described with the same accuracy by these MO's.
The Configuration Interaction calculation included 175
configurations. The vibrational eigenfunctions, energies
and integrals were calculated by numerical integration.
Selection of the ground state vibration functions, that
have the correct energy to interact with an excited state
level, was performed by a procedure based on the back-
tracking algorithm. The diagonalization of the interaction
matrix and the time-dependent interference of the result-
ing eigenstates were calculated numerically.
The calculation of the $S_0 \rightarrow S_1$ radiative transition with the
ABO set gives good correspondence with the experiment; the

results obtained with the CBO set give no correspondence
with the experiment.

The calculation of the radiationless $S_1 \rightarrow S_0$ transition of
formaldehyde with the ABO set indicates that this molecule
belongs to the so-called resonance case; this means that
an excited state level couples with so few levels of the
ground state, that an oscillatory behaviour of the oscilla-
tor strength results; the oscillation times are of the
order of 10^{-11} seconds and are therefore not experimentally
detectable. The experimentally found exponential decay can
thus not be explained by the internal conversion process
as has been assumed; it can in principle be explained by
taking into account the coupling of the excited state
with the dissociative continuum levels.

SAMENVATTING

In Hoofdstuk 1 worden de voorwaarden onderzocht
waaraan 'n basisset moet voldoen om stralingsloos verval
te kunnen beschrijven. Deze voorwaarden worden afgeleid
door te onderzoeken welke voorwaarden gesteld moeten wor-
den aan de exacte vergelijkingen voor het proces om deze
te laten vereenvoudigen tot een gegeneraliseerde vorm van
het Bixon-Jortner model voor stralingsloos verval.
In de andere hoofdstukken wordt de *ab initio* berekening
van de $S_1 \rightarrow S_0$ stralings- en stralingsloze overgang in for-
maldehyde beschreven.
De berekening van het stralingsloze proces in formaldehyde
werd gedaan met twee basissets: de Adiabatische Born
Oppenheimer basisset en de Crude Born Oppenheimer basisset.
De koppeling in de ABO set werd berekend door de koppeling
uit te drukken in integralen over de elektrische veld-
operator. Het zes-dimensionale potentiaaloppervlak voor de
kernbeweging werd benaderd door zes doorsneden volgens de
normaalcoördinaten. De elektronengolffunctie werd berekend
met een Gaussische AO set van dubbel-zeta kwaliteit. De
SCF MO's werden berekend met een gemodificeerde Hartree-
Fock operator: de Transition operator; dit om ervoor te
zorgen dat de grond- en $(n\pi^*)$-aangeslagen toestand met
dezelfde nauwkeurigheid worden beschreven door deze MO's.
De Configuratie Interactie berekening had betrekking op
175 configuraties. De vibrationele eigenfuncties, -ener-
gieën en -integralen werden berekend door numerieke inte-
gratie. De selectie van de grondtoestand vibratiefuncties,
die de juiste energie hebben om een interactie aan te
gaan met een niveau van de aangeslagen toestand, werd ver-
richt met een procedure gebaseerd op het backtracking
algoritme. De diagonalisatie van de interactie matrix en
de tijdafhankelijke interferentie van de resulterende

eigentoestanden werden numeriek berekend.

De berekening van de $S_0 \rightarrow S_1$ stralingsovergang met de ABO
set geeft goede overeenkomst met het experiment; de resul-
taten verkregen met de CBO set geven geen overeenkomst met
het experiment.

De berekening van de stralingsloze $S_1 \rightarrow S_0$ overgang in for-
maldehyde met de ABO set geeft aan dat dit molecule tot
het zogenaamde resonantiegeval behoort; dit betekent dat
een niveau van de aangeslagen toestand met zó weinig ni-
veau's van de grondtoestand koppelt, dat een oscillerend
gedrag van de oscillatorsterkte resulteert; de oscillatie-
tijden zijn van de orde van 10^{-11} seconde en zijn daarom
experimenteel niet meetbaar. Het experimenteel gevonden
exponentiële verval van de oscillatorsterkte kan daarom
niet verklaard worden met het interne conversieproces zoals
werd aangenomen; het kan in principe wèl verklaard worden
door de koppeling van de aangeslagen toestand met de
dissociatieve continuumniveau's in rekening te brengen.

CURRICULUM VITAE

De schrijver werd op 25 september 1951 geboren in
Eindhoven. Na het behalen van het einddiploma HBS-B aan
het Sint Joriscollege te Eindhoven werd in 1968 begonnen
met de studie aan de afdeling der Scheikundige Technologie
van de TH Eindhoven. In 1971 werd het kandidaatsexamen
met lof afgelegd. Het afstudeeronderzoek werd verricht
onder leiding van prof. dr. H.M. Buck bij de vakgroep
Organische Chemie. In september 1973 werd de studie afge-
sloten door het met lof afleggen van het doctoraal-
examen. In september 1973 werd hem de Unileverprijs toe-
gekend. In oktober volgde aanstelling als wetenschappelijk
ambtenaar in de vakgroep Organische Chemie en werd met het
onderzoek, beschreven in dit proefschrift, begonnen.
Het volgen van de "Charles Coulson Summer School" te
Oxford in 1974 en het "Summer Institute" van prof. P.O.
Löwdin in Uppsala in 1975 heeft een waardevolle bijdrage
geleverd tot zijn studie in de theoretische chemie. Per
1 december 1977 zal hij in dienst treden als wetenschap-
pelijk medewerker bij het Philips' Natuurkundig Labora-
torium te Eindhoven.

STELLINGEN

1. Het door Bernardi *et al.* gegeven mechanisme voor sigmatrope
   verhuizing van halogeen atomen houdt geen rekening met de
   inversie van de bindende orbital.

   > F. Bernardi, N.O. Epiotis, R.L.
   > Yates, J. Am. Chem. Soc., 97,
   > (1975), 1334

2. De set van standaardmoleculen gebruikt om de parameterset
   voor fluor in de MINDO/3 methode af te leiden, is te beperkt.

   > R.C. Bingham, M.J.S. Dewar, D.H.
   > Lo, J. Am. Chem. Soc., 97 (1975),
   > 1307

3. Het verdient aanbeveling om de invloed van de Born-Oppen-
   heimer koppeling op rotatiedispersie te onderzoeken.

4. Aan de invloed van de dispersiegraad van legeringskatalysa-
   toren op de selectiviteit moet meer aandacht besteed worden.

5. Het Ingold mechanisme voor intramoleculaire electron shifts
   kan gecombineerd met het concept van "conservation of
   orbital symmetry" leiden tot een gedetailleerde beschrijving
   van het mechanisme van intramoleculaire reacties.

   > P. Schipper, Thesis (1977),
   > Eindhoven

6. Het verdient aanbeveling om fosforanylradicalen met C_{4v}-
   symmetrie te onderzoeken, omdat zij een overgang vormen
   tussen die met D_{3h}- en T_d-symmetrie.

   > G. Boekestein, Thesis (1975),
   > Eindhoven

7. Parapsychologie beoefend door psychologen is hetzelfde als chemie beoefend door agogen.

8. Parapsychologen die verklaren dat telepathie in principe niet verklaard kan worden met de huidige natuurwetenschappen, zijn of totaal onwetend over de werking van de televisie of achten een televisie ingewikkelder dan een mens.

9. Het is vreemd dat het gezondheid-ondermijnende beroep van topsporter geen aanleiding heeft gegeven tot wettelijke maatregelen ter bestrijding hiervan.

10. Bij de promotieplechtigheid aan de Technische Hogeschool Eindhoven wordt het raadplegen van de paranimfen in ernstige mate gehandicapt door het feit dat zij in de zaal moeten zitten.

> Artikel 2, protocol promotiezitting, TH Eindhoven

11. De praktijk van de WUB heeft nogmaals de "ijzeren wet van de oligarchie" bevestigd.

> R. Michels, "Zur Soziologie des Parteiwesens in der modernen Demokratie"

12. In het algemeen wordt aan artikel 17, lid 2 van het promotiereglement van de Technische Hogeschool Eindhoven weinig de hand gehouden.

> Uitspraak van ir. W.A.M. Castenmiller

J.M.F. van Dijk   Eindhoven, 15 november 1977